Using terrestrial laser scanning to constrain forest ecosystem structure and functions in the Ecosystem Demography model (ED2.2)

Félicien Meunier[1], Sruthi M. Krishna Moorthy[1], Marc Peaucelle[1], Kim Calders[1], Louise Terryn[1], Wim Verbruggen[1], Chang Liu[1], Ninni Saarinen[2,3], Niall Origo[4], Joanne Nightingale[4], Mathias Disney[5,6], Yadvinder Malhi[7], Hans Verbeeck[1]

[1]Computational and Applied Vegetation Ecology, Department of Environment, Ghent University, Ghent, Belgium
[2]Department of Forest Sciences, University of Helsinki, ~~Ghent,~~ Finland
[3]School of Forest Sciences, University of Eastern Finland, Finland
[4]NPL, Climate and Earth Observation (CEO) group, National Physical Laboratory, Teddington, UK
[5]Department of Geography, UCL, Gower Street, London WC1E 6BT, UK
[6]NERC, National Centre for Earth Observation (NCEO), UCL Geography, Gower Street, London, WC1E 6BT, UK
[7]Environmental Change Institute, School of Geography and the Environement, University of Oxford, Oxford, UK

Correspondence to: Félicien Meunier (Felicien.Meunier@ugent.be)

Abstract. Terrestrial Biosphere Modeling (TBM) is an invaluable approach for studying plant-atmosphere interactions at multiple spatial and temporal scales, as well as the global change impacts on ecosystems. Yet, TBM projections suffer from large uncertainties that limit their usefulness. A large part of this uncertainty arises from the empirical allometric (size-to-mass) relationships that are used to represent forest structure in TBMs. Forest structure actually drives a large part of TBM uncertainty as it regulates key processes such as the transfer of carbon, energy, and water between the land and atmosphere, but remains challenging to measure and reliably represent. The poor representation of forest structure in TBMs results in models that are able to reproduce observed land fluxes, but which fail to realistically represent carbon pools, forest composition, and demography. Recent advances in Terrestrial Laser Scanning (TLS) techniques offer a huge opportunity to capture the three-dimensional structure of the ecosystem and transfer this information to TBMs in order to increase their accuracy. In this study, we quantified the impacts of integrating structural observations of individual trees (namely tree height, leaf area, woody biomass, and crown area) derived from TLS into the state-of-the-art Ecosystem Demography model (ED2.2) at a temperate forest site. We assessed the relative model sensitivity to initial conditions, allometric parameters, and canopy representation by changing them in turn from default configurations to site-specific, TLS-derived values. We show that forest demography and productivity as modelled by ED2.2 are sensitive to the imposed initial state, the model structural parameters, and the way canopy is represented. In particular, we show that: 1)

- the imposed openness of the canopy dramatically influenced the potential vegetation, the optimal ecosystem leaf area, and the vertical distribution of light in the forest, as simulated by ED2.2; 2)
- ~~–~~ TLS-derived allometric parameters increased simulated leaf area index and aboveground biomass by 57 and 75%, respectively; 3)

- the choice of model structure and allometric coefficient both significantly impacted the optimal set of parameters necessary to reproduce eddy covariance flux data.

We conclude that integrating vegetation structure information derived from TLS can inform TBMs on the most adequate model structure, constrain critical parameters, and prescribe representative initial conditions. Our study also confirms the need for simultaneous observations of plant traits, structure and state variables if we seek to improve the robustness of TBMs and reduce their overall uncertainties.

1 Introduction

Terrestrial biosphere models (TBMs) are key tools to understand the ecosystem response to anthropogenic disturbances and climate change (Medvigy and Moorcroft 2012; McGuire et al. 2001). Nowadays they are intensively used, as is or embedded in Earth system models, to study plant-atmosphere interactions and predict the future of ecosystems facing global change (*e.g.,* Poulter et al. 2010). Yet, the usefulness of TBMs are currently limited by the large uncertainties in their projections which originate from different sources (Lin et al. 2011).

Forest structure has long been recognized as a critical component to understand forest dynamics (Hurtt et al. 2010). It influences the climatically important fluxes of carbon, energy, and water (Bonan 2008). Yet, its realistic representation is complex, challenging and an urgent priority in the development of next-generation TBMs (Fisher et al. 2018). The representation of the forest structure within TBMs is associated with three sources of uncertainty: the model structure, the initialization, and the parameter uncertainty.

The model structure entails by definition all the processes included in a model, how they are implemented, and all the underlying assumptions (Bonan 2019). Model structure complexity varies among TBMs and also depends on the user configuration choices: different formulations of the same process can co-exist within a TBM. This complexity results from the necessary compromise between an accurate representation of the reality on the one hand and the computational demand and observational requirements on the other (Shiklomanov et al. 2020). Model intercomparison studies have demonstrated that discrepancies in the representation of key processes such as forest structure (Fisher et al. 2018) or photosynthesis (Rogers et al. 2017) lead to significant uncertainties in the projections of critical variables such as the overall land carbon sequestration capacity (Friedlingstein et al. 2014; Lovenduski and Bonan 2017; Friedlingstein et al. 2006).

The initialization uncertainty reflects the error made when determining the initial conditions of the modelled ecosystem. Several approaches exist for initializing TBMs, the most common of which is probably to start runs from near-bare ground conditions, force the simulations with relevant climate-forcings, and wait for the model to reach an equilibrium state, the so-called potential vegetation (Antonarakis et al. 2011). Yet, such a spin-up approach does not guarantee reliable initial demography, carbon pools or ecosystem structure. Alternatively, forest inventories can be used to prescribe the initial composition of the ecosystem (Medvigy et al. 2009). The derivation of the initial states of critical variables, such as the

aboveground biomass or the total leaf area from the plant size distribution, then relies on model default allometries which are often derived from other, potentially non-representative site-specific data.

Parameter uncertainty arises e.g. from the necessary simplification of the natural complexity into a coherent model structure, the uncertainty in the measurements used to calibrate the model, or the methods used to upscale local measurements to scales on which TBMs operate (Zaehle et al. 2005). Previous sensitivity analyses have underlined the critical importance of parameter uncertainty for the projections of ecosystem demography and productivity (Dietze et al. 2014; Massoud et al. 2019; Raczka et al. 2018; Wramneby et al. 2008). In a recent comparative study, parameter uncertainty was even shown to drive the overall model uncertainty (Shiklomanov et al. 2020). Among model parameters, allometric coefficients scale the shape and mass of the plants or of its components with their size (Chave et al. 2014). Not surprisingly, multiple TBMs were shown to be sensitive to such allometric parameters (Collalti et al. 2019; Cano et al. 2020; Esprey et al. 2004). Parameter uncertainty can be reduced by constraining the range of variation of model parameters through the assimilation of different sources of observations or via model optimization (LeBauer et al. 2013). In the past, TBMs have often been calibrated with eddy covariance data (Fer et al. 2018; Rezende et al. 2016; Collalti et al. 2016). While this approach ensures that the model correctly reproduces the short timescale (diurnal/seasonal) dynamics of land fluxes, it does not ensure an accurate representation of forest structure and carbon pools. This is especially true because forest structure-related parameters can present a low sensitivity to those observations (LeBauer et al. 2013; Richardson et al. 2010), and the large equifinality in TBMs (Luo et al. 2009) can lead to acceptable land fluxes with a poor representation of ecosystem structure (i.e. fluxes can be reproduced from an almost infinite range of structural possibilities, some of which will be much more likely that would be others).

Among the different sources of observations used to reduce model uncertainties, remote sensing from various platforms (terrestrial, air- and space borne) has increasingly been used to monitor and understand vegetation ecosystems (Jones and Vaughan 2010). The recent revolution in Terrestrial Laser Scanning (TLS, also called terrestrial LiDAR) provides new opportunities for constraining TBMs, and reducing the uncertainties related to the vegetation structure representation (Fischer et al. 2019). The ability of TLS to measure the distance to reflecting surfaces was initially used in ecological studies to measure simple metrics like DBH and tree heights (Maas et al. 2008; Hopkinson et al. 2011). Since then, TLS methods have rapidly evolved to derive more complex metrics, such as the vertical profiles of the forest structure (Jupp et al. 2009; Calders et al. 2018) and whole-tree volumetric assessments (Fan et al. 2020), leading to an accurate representation of forest structure across various forest types (Calders et al. 2015; Tanago et al. 2018; Takoudjou et al. 2018; Ehbrecht et al. 2017; Stiers et al. 2018; Saarinen et al. 2021.). Today, the ability of TLS to accurately represent the 3D structure of forests via quantitative structure modelling or QSM (Raumonen et al. 2013; Hackenberg et al. 2015) represents a huge opportunity to improve our understanding of forest ecosystems under changing climates (Calders et al. 2020). In particular, TLS snapshots of vegetation ecosystems could simultaneously provide important state variables to initialize TBMs, strong constraints to some critical allometric parameters, and help determine the most appropriate model structure for key processes.

In this study, we quantified the sensitivity of a specific TBM, ~~namely~~ the Ecosystem Demography model version 2 (ED2.2), to vegetation structure by varying the initial state of the modelled ecosystem and the model allometric parameters that control the structural representation of the canopy within the model. More specifically, we investigated the benefits of integrating TLS measurements of forest structure on the simulated demography and productivity, as well as on the model calibration when using flux tower data. We were particularly interested to: (i) assess the relative importance of model structure, initialization, and parameter uncertainties in the ED2.2 model in a temperate forest; (ii) quantify the potential added value of TLS data for vegetation modelling (as, to the best of our knowledge, this study is the first attempt to couple TLS data and a TBM); and (iii) determine if equifinal ecosystem simulations could be discriminated from a structural point of view.

2 Material and Methods

2.1 Study site and data

2.1.1 Study site

Wytham Woods is a mixed deciduous forest, predominantly broadleaved, covering approximately 40 ha. It is located 5 km northwest of Oxford in southern England (Thomas et al. 2011). Owned by Oxford University, Wytham Woods has been part of the UK Environmental Change Network (ECN) and of the Smithsonian Global Earth Observatory (SIGEO) Network since 1992 and 2008, respectively, and has hosted numerous ecological studies (Savill et al. 2010). The site is classified as an ancient semi-natural woodland (Hall et al. 2001). This classification means that the site has been continuously covered by trees through recorded history (since at least 1600), occasionally managed, and experienced minimum intervention (i.e. no silvicultural management) since WWII (Fenn et al. 2015). Over the 1993-2008 time period, the site was characterized by a mean annual temperature of 10°C and a mean annual precipitation of 726 mm (Butt et al. 2009). The study took place on a 1.4 ha forest plot nested within the 18 ha long-term monitoring site part of the ForestGEO global network of forest inventory plots. This 140 × 100 m area has a local SW-coordinate (0, 100) and local NE-coordinate (140, 200) boundary. The local origin coordinate (0,0) was measured with a differential GPS and located at Lat 51.7750579, Lon -1.33904729.

2.1.2 Field inventory and Terrestrial Laser Scanning data

The studied plot was inventoried during the summer of 2016. All trees were located, measured, and identified at the species level. The plot is largely dominated by sycamore (Acer pseudoplatanus, 65% of the 821 inventoried trees in the 1.4 ha plot, see Table 1 and Figure 1), ash (Fraxinus excelsior, 10%), and hazel (Corylus avellana, 8%). Oaks (Quercus robur) represent a limited fraction of the woody stems (4%) but disproportionately contribute (23%) to the total basal area (BA) as they mostly consist of large trees (Table 1 and Figure 1). The mean (resp. median) DBH is 24.4 (resp. 19.8) cm, ranging from 2.9 cm to 141.2 cm.

Three-dimensional forest structure data were collected using a RIEGL VZ-400 terrestrial laser scanner (RIEGL Laser Measurement Systems GmbH) in leaf-on (June and July 2015) and leaf-off (December 2015 and January 2016) conditions (Calders et al. 2018). The RIEGL instrument uses on-board waveform processing and records multiple return LiDAR data, which improves vertical sampling (Lovell et al. 2003; Calders et al. 2014). Individual trees were extracted using treeseg (Burt, et al. 2019), and their structure modelled with TreeQSM (Raumonen et al. 2013) with the leaf-off TLS point cloud. Leaves were then added to the individual tree branches using both the leaf-off and -on TLS datasets. Doing so, TLS allowed retrieving of individual tree height, aboveground woody biomass (modelled through estimates of volume combined with species-specific wood density), and leaf area. In addition, the individual tree crown area was computed from the vertical projection of the leaf-off point clouds of individual trees. For more details, a complete description of the TLS data collection and forest stand reconstruction is available in Calders et al. (2018).

2.1.3 Flux tower data and species traits

Stand-scale carbon and water fluxes have been occasionally measured in Wytham Woods using the eddy covariance technique. We digitized the most recent (to our knowledge) data collection of CO2 flux that was reported by Thomas et al. (2011) for the period between May 2007 and April 2009. To do so, we digitized the weekly mean values of ecosystem gross primary productivity (GPP), ecosystem respiration (Reco) and net ecosystem productivity (NEP) from Figure 6 of the aforementioned reference using the Plot digitizer software (v.2.6.8, http://plotdigitizer.sourceforge.net/).

In addition, we extracted all existing records of specific leaf area (SLA) and maximum rate of carboxylation (V_{cmax}) for the five most important species in Wytham woods from the TRY database (Kattge et al. 2020), see Table 1 (the complete list of references used is available in Appendix). Individual traits were converted into ED2.2 units ($m^2\ kg_C^{-1}$ for SLA with a constant leaf carbon content of 0.5 and $\mu mol_C\ m^{-2}\ s^{-1}$ for V_{cmax}). V_{cmax} data were also rescaled to the ED2.2 reference temperature (15°C) using the model default value for the temperature coefficient Q10. Following Asner et al. (2017), we calculated the community-weighted mean (CWM) and community-weighted standard deviation (CWSD) for both traits based on the species composition and species-level average values, using species basal area as weights:

$$CWM = \frac{\sum_{i=1}^{N} w_i \cdot x_i}{\sum_{i=1}^{N} w_i} \quad (1)$$

$$CWSD = \sqrt{\frac{\sum_{i=1}^{N} w_i \cdot (x_i - CWM)^2}{\frac{(N-1)\sum_{i=1}^{N} w_i}{N}}} \quad (2)$$

where N is the total number of species for which data was available in TRY for trait x, x_i is the mean trait value for species i, and w_i is its weight (here, the total basal area of species i). Those trait data were not used to calibrate nor validate the model as such but ~~simply~~ simply compared with the optimized parameters after calibration (see below).

2.2 Model

2.2.1 The terrestrial biosphere model ED2.2

ED2.2 is a terrestrial biosphere model that can simulate the vegetation dynamics of a wide range of ecosystems from boreal to tropical forests (Longo et al. 2019). It is a cohort-based, spatially implicit model that approximates the behavior of an individual-based, spatially distributed vegetation model through a system of size- and age-structured partial differential equations (Moorcroft et al. 2001). ED2.2 integrates modules of plant growth, mortality, phenology, disturbance, hydrology, and soil biogeochemistry to predict e.g., the demography, the succession, and the dynamics of water and carbon within the simulated ecosystem.

In ED2.2, the inter- and intra-specific diversity is represented by a set of plant functional types (PFTs) that differ by their leaf physiology, phenology, growth and allocation strategies, mortality, and sensitivity to environmental conditions. All trees inventoried in Wytham Woods were classified as mid-successional temperate deciduous trees. This PFT is cold-deciduous, i.e. leaf phenology is prognosed by the accumulation of growing degree-days and chilling days during the extended growing and senescing season, respectively (Longo et al. 2019).

By default in ED2.2, plant canopies are represented as infinitely thin flat crowns (a.k.a. complete shading) that virtually occupy the entire horizontal space of the patch in which the cohort is located. In an alternative configuration, cohorts are stacked on top of each other but have finite radius and hence tallest plants only partially shade the underlying cohorts. A comprehensive model description (including photosynthesis, radiative transfer, and phenology) is available in Longo et al. (2019).

2.2.2 Model default and TLS-derived allometries

In ED2.2, the carbon made available from net assimilation is partitioned at the cohort level into the different plant pools according to DBH-dependent allometries (Longo et al. 2019). In other words, plant cohorts allocate the carbon assimilated through photosynthesis to living tissues (i.e. fine roots, sapwood, leaves, seeds), the non-structural storage pool, and the dead tissues (i.e. coarse roots, and aboveground woody biomass) depending on (i) a set of allometries and (ii) whether the plant carbon balance and environmental conditions are favorable for growth. As such in ED2.2, aboveground woody biomass, height, leaf biomass, and crown area are scaled through DBH-dependent allometries (Table 2). The ED2.2 default allometric parameters are defined according to Medvigy et al. (2009) for the leaf biomass and height, Dietze et al. (2008) for the crown area, and Albani et al. (2006) for the aboveground woody biomass.

We compared those default allometric parameterization with site-specific, TLS-derived ones. To do so, we fitted the individual plant metrics (height, crown area, aboveground woody biomass, and leaf area) vs DBH relationships derived from TLS using the ED2.2 default set of equations (Table 2). More specifically, the parameters of the four allometric equations of the ED2.2 model were optimized with the 'nlsLM' function of the minpack.lm R package (Elzhov et al. 2016) for the height and the 'lm' function of the 'stats' R package applied to the log-transformation of the allometric power equations for the crown area, the leaf biomass, and the aboveground woody biomass. To convert the leaf area obtained from TLS into leaf biomass, we used the CWM of SLA.

2.2.3 Model initialization and forcings

In this study, the ED2.2 model was initialized using i) near-bare ground initial conditions (i.e. seedlings only), ii) the DBH distribution available through the field inventory, or iii) the TLS-reconstructed size distribution. In the latter two configurations, the 1.4 ha site was initially divided into 35 square patches of 20 x 20 m ~~that were allowed to fuse along the simulation~~. Simulations were run for multiple years using the corresponding years of the CRU-NCEP reanalysis forcing dataset (Viovy 2018).

2.3 Analyses

To achieve the overarching objective of this study, we designed three different main analyses that explore the sensitivity of the model to TLS data. Those analyses aim to compare the potential vegetation, the forest structure and its functioning, as well as the model calibration between the default model configuration and when the model is informed by TLS data. The overall workflow of this study together with the three main analyses are schematically represented in Figure 2.

2.3.1 Impact of TLS data on model allometries and initial conditions

We first compared the model default allometries with the site-specific ones derived from the TLS data. To do so, we evaluated the quality of fit of both allometric models by computing the corresponding mean relative errors (van Breugel et al. 2011) for all four considered allometric metrics. To assess the relative importance of TLS for the model initialization, we compared the tree size distributions obtained from the field inventory and from the TLS data using a linear model and by computing the absolute and relative differences between both DBH distributions.

2.3.2 Sensitivity of the potential vegetation to TLS data (Analysis I)

To evaluate the impact of TLS data on potential vegetation, we compared uncalibrated simulations, initialized from near-bare ground (NBG) conditions and run for 100 years, which approximately corresponds to the latest large-scale disturbance (Analysis I). We specifically considered three model configurations: the model default (NBG-Default), the finite crown (NBG-FC), and one constrained with TLS data (NBG-TLS). NBG-Default represents the most traditional version of ED2.2. It uses the ~~model~~ default coefficients for all allometric equations and the default infinite size representation of tree crowns.

NBG-FC is identical to NBG-Default, except for the finite crown (FC) representation. Finite crowns are expected to increase light availability for short cohorts by reducing the light intercepted by the tallest ones (Dietze et al. 2008). Finally, NBG-TLS was configured according to the allometric coefficients fitted to the TLS data for the individual plant height, the leaf biomass, the aboveground woody biomass, and the crown area. Table 4 summarizes all model configurations used in this study alongside with their most important features. To evaluate the impact of the model structure and TLS-derived allometries, we compared the size distribution of the potential vegetations as simulated by ED2.2 for the three model configurations with the inventory data.

2.3.3 Short-term model sensitivity to TLS-derived allometries (Analysis II)

To quantify the impact of TLS-derived allometries on ED2.2 outputs at short-time scales, we ran a batch of sixteen uncalibrated sensitivity analysis (SA) simulations prescribed with field inventory data (Analysis II). In those simulations, we progressively incorporated the allometric parameters optimized from the TLS data, by changing a single or a combination of allometric equations from the default set of relationships. We then compared the relative changes of some of the most relevant model outputs (i.e., the ecosystem GPP, the total leaf area index (LAI), the understorey photosynthetically active radiation (PAR), and the aboveground woody biomass) between the sensitivity analysis runs and a reference one that used all default allometric parameters. In this analysis, we calculated those relative changes as the direct or the indirect impact of each allometric equation. The direct impact corresponds to the effect of changing a single allometric equation from the default model parameterization while the indirect impact reflects the incremental effect when changing an additional allometric equation in a combination.

2.3.4 Parameter data assimilation and model equifinality (Analysis III)

Finally, we also investigated the impact of TLS data on model calibration. To do so, we repeated a parameter optimization by Bayesian data assimilation for another set of three model configurations (Analysis III). The model configurations included a default model version (default allometric parameters, infinite crown area), and a finite crown representation (default allometric parameters, finite crown radius), which were both initialized with field inventory data, as well as a TLS informed configuration (TLS-derived allometric parameters, finite crown radius), whose initial condition was prescribed with the TLS size distribution. These three model setups are here-after referred to as IC-Default, IC-FC, and IC-TLS and are again fully detailed in Table 4.

More precisely, we optimized a set of two parameters (SLA and V_{cmax}) according to the IC-Default, IC-FC, and IC-TLS model setups. In ED2.2, SLA is used to convert the leaf biomass into leaf area. Therefore, it strongly regulates the radiative transfer within forest patches and hence mediates light competition between cohorts. The maximum rate of carboxylation V_{cmax} is one of the most important drivers of plant net assimilation, and hence determines the carbon available for each cohort (Dietze et al. 2014; Longo et al. 2019). Those two parameters are excellent candidates to calibrate the ecosystem's

land fluxes and are often used to do so, including in ED2.2 (Camino et al. 2019; Fer et al. 2018; Rezende et al. 2013; Sakschewski et al. 2015; Tan et al. 2010).

Model calibrations were achieved within the Predictive Ecosystem Analyzer (PEcAn), an ecological workflow management software (LeBauer et al. 2013). Specifically, the Bayesian emulator framework developed by Fer et al. (2018) was used to optimize the parameter set to the two years of GPP data. For the calibration, we only used the GPP flux, letting aside the Reco and NEP data, as we focus here on plant parameters calibration. Using Reco and/or NEP would have necessitated the additional tuning of respiration parameters, which was beyond the scope of this study. The emulator approach replaces computationally expensive models such as ED2.2 by a statistical model compatible with Markov chain Monte Carlo (MCMC) chains algorithms. It consists in a statistical model constructed by interpolating the response curve between the knots (i.e. the points where the model goodness of fit was previously evaluated). The Emulator calibration was systematically run in three rounds, each with 100,000 iterations of three MCMC chains, using a total of 300 knots (100 per round). After calibration, we ran ensemble runs of 100 members for three years for each configuration, with SLA and V_{cmax} sampled from the posterior distribution generated by the emulators. We used uninformative uniform distributions covering all trait data from TRY as priors for both parameters (Table 3).

3 Results

3.1 Impact of TLS data on model allometries and initial conditions

Individual tree measurements from QSMs applied to the TLS point cloud could all be satisfactory represented by ED2.2 allometric equations (Figure 3). R^2 of the allometric models for the individual aboveground woody biomass, height, crown area, and leaf biomass respectively reached 0.95, 0.83, 0.67, and 0.77. The mean relative errors changed from -46.9 to 1.42% (woody biomass), from 14.7 to -4.8% (height), from 109.0 to 9.1% (crown area), and from -26.8% to 2.8% (leaf biomass) when switched from ED2.2 default allometries to TLS-derived, site-specific ones.

Over the DBH range in Wytham Woods, TLS-derived allometric coefficients led to systematically larger allocations to aboveground woody biomass (+73% on average, up to +177% for the smallest tree) and leaf biomass (+75% on average), and smaller tree height (-1.9 m on average) as compared to ED2.2 defaults (Figure 3). Individual crown areas derived from TLS measurements varied between 0.2 and 465.4 m², with a mean of 26 m². As compared to the TLS-calibrated allometry, default model parameters predicted larger crown areas for trees with DBH < 64 cm (-22% on average), and smaller crown areas for trees with DBH ≥ 64 cm (+17% on average). The latter category (DBH ≥ 64 cm) comprised 30 trees (3.7% of the total) and contributed to 30.7% of the total basal area.

TLS-derived and field inventory DBHs were well correlated (R^2 = 0.98, RMSE = 2.3 cm, slope of the inventory vs TLS linear model = 0.998, see supplementary Figure S1). The mean (resp. median) relative difference between the TLS and field inventory DBHs was -0.2% (resp. -1.7%). The minimum and maximum difference in DBH reached -13.8 and 32.9 cm, respectively (Supplementary Figure S2).

3.2 Sensitivity of the potential vegetation to TLS data (Analysis I)

None of the unprescribed simulations (NBG-Default, NBG-FC and NBG-TLS) captured the size distribution observed through the inventory (Figure 6). While the infinite crown configuration (NBG-Default) generated large trees (DBH > 70 cm), yet smaller than the observations (the biggest tree cohort in the NBG-Default reached 74.4 cm in DBH while the biggest tree based on the field inventory had a DBH of 127.4 cm), it systematically underestimated the density of small (DBH < 50 cm) trees, by 46% on average. The opposite trend could be observed for both configurations with finite crowns (NBG-FC and NBG-TLS), with a smaller density of large trees when allometric coefficients were derived from TLS data (NBG-TLS). When starting from near-bare ground conditions, model structure (NBG-FC vs NBG-Default, +53% on average) had a bigger impact on the tree size distribution than the allometric coefficients (NBG-TLS vs NBG-FC, -7% on average), see Figure 4.

3.3 Short-term model sensitivity to TLS-derived allometries (Analysis II)

Direct and indirect impacts of TLS-derived allometries were well correlated for every model output considered (the slope of the linear model of all indirect vs all direct impacts = 0.96, R^2 = 0.96). Direct and indirect impact systematically agreed on the direction of the output changes and only slightly changed in magnitude (1.5% on average across all outputs and allometries) when allometric equations were considered alone or in combination with one another (Figure 5).

Leaf biomass allometry as derived from TLS had the largest impact on the simulated LAI (+57% for the direct effect) and consequently on ecosystem GPP (+21%). Those simulated increments can be explained by the larger carbon allocation to leaves (Figure 3). The large variability around those mean relative changes are due to the large fluctuations between the winter (leaf-off season for the reference as well as the sensitivity runs) and the summer (leaf-on season, LAI and GPP respectively increased on average by 91% and 50% in the sensitivity runs).

The simulated aboveground woody biomass was mostly sensitive to the wood biomass allometry parameters. The consistently larger allocation to woody biomass induced by the use of TLS data (Figure 3) resulted in a 75% increase in ecosystem carbon storage in aboveground dead tissues. Yet, it did not influence any of the other model outputs (Figure 5) as that carbon pool is mainly inert and does not influence a lot of processes downstream.

The updated crown area allometry reduced ecosystem LAI and hence its GPP. That was due to the reduction in crown area for most simulated trees induced by the use of TLS-derived allometries (Figure 3), which reduced individual tree light interception, and as a result, increased light availability in the understory (by 7% on average) while leaf development and tree productivity decreased by -2% and -5%, respectively.

3.4 Parameter data assimilation and model equifinality (Analysis III)

All three model configurations for which parameters were calibrated (IC-Default, IC-FC, and IC-TLS) were able to capture both the amplitude and the seasonality of the gross ecosystem productivity, as observed by the eddy covariance flux tower

(Figure 6). The posterior ensemble runs from calibrated configurations (IC-Default, IC-FC, and IC-TLS) were almost indistinguishable in terms of goodness of fit. R^2 of observed vs modelled monthly GPP reached 0.94 for all three configurations (Figure 6A) while the RMSE varied between 0.1 (IC-Default) and 0.3 (IC-TLS) µmol m^{-2} s^{-1}, much lower than the mean and standard deviation of the two years of observational data of GPP (5.5 and 4.7 µmol m^{-2} s^{-1}, respectively). Because we only simulated one fully deciduous PFT, the model underestimated GPP during the winter: simulated ecosystem LAI and hence gross assimilation dropped down to zero from January to March while measured ecosystem productivity was non-null during the same period (Figure 6B) due to understorey plants (such as shrub not simulated here).

Despite the similarities in simulated GPP, those runs resulted in very different parameter posterior distributions (Figure 7). When infinitely wide crowns were simulated (IC-Default), predicted median SLA (14.4 m^2 kgC^{-1}) was lower than the CWM (25.1 m^2 kgC^{-1}), the model default (24.3 m^2 kgC^{-1}), and the posterior median of the two configurations with a finite crown representation (36.9 and 26.8 m^2 kgC^{-1} for IC-FC and IC-TLS, respectively), see Tables 1 and 3. Contrastingly, posterior median V_{cmax} of the IC-Default configuration (47.3 µmol m^{-2} s^{-1}) was considerably larger than the ED2.2 default (17.5 µmol m^{-2} s^{-1}), the CWM (32.6 µmol m^{-2} s^{-1}), and than in the other two configurations (13.2 and IC-TLS 16.7 µmol m^{-2} s^{-1} for IC-FC and IC-TLS, respectively).

Modelled GPP was sensitive to both SLA and V_{cmax} with a slightly higher responsiveness to SLA (Supplementary Figure S3). SLA was therefore the primary driver of the cost function to evaluate the model fitness, and was negatively correlated with V_{cmax} (Table 3). The IC-TLS configuration resulted in the posterior median SLA that was the closest to the CWM (26.9 vs 25.1 m^2 kgC^{-1}) while calibrated V_{cmax} in the IC-TLS and IC-Default configurations were equidistant to the CWM (Figure 7).

3.5 TLS-derived impacts on ecosystem structure and functions

Simulated ecosystems were all characterized by contrasting structures and functioning as a result of the discrepancies between configurations and parameterization. Both the model structure and the allometric coefficients had large impacts on critical model outputs. The ecosystem LAI of the IC-Default configuration was smaller (1.8 m^2 m^{-2} on average during the leaf-on season) compared to other prescribed model runs (4.5 m^2 m^{-2}~~$m2$ $m-2$~~) and the range of observations in the literature (3.6 - 4.1 m^2 m^{-2}~~$m2$ $m-2$~~), see Table 5. Yet despite smaller leaf areas, the infinitely wide crowns configuration (IC-Default) made the forest more opaque to the incoming solar radiation than the other calibrated configurations (IC-FC and IC-TLS): the PAR available in the understorey decreased by 14%. When comparing prescribed model configurations with finite crown areas (IC-FC and IC-TLS), the smaller carbon allocation to leaves imposed by ED2.2 default allometries (Figure 3) was compensated by the larger calibrated values of SLA (Figure 7) resulting in a similar total ecosystem leaf area (Table 5) and its vertical distribution (Figure 8) after calibration. Similarly, the LAI of the potential vegetation simulated from near bare-ground configurations was 32% higher with infinite crowns, but at the same time 14% less PAR reached the understorey (Table 5).

As the soil received more radiation when finite crowns were simulated, it was warmer and as a result, heterotrophic (and ecosystem respiration) largely increased (+26% on average) when switching from closed to finite crowns (Table 5). Forest

carbon stocks also diverged between configurations: driven by higher allocations to leaf and aboveground woody biomass, aboveground carbon storage was much larger (+70% on average) in TLS-derived runs (NBG-TLS and IC-TLS) than when default allometries were applied (Table 5). Estimates of aboveground woody biomass from configurations starting from near bare-ground conditions were also contrasted but systematically lower than the TLS estimates (23.9 kg_C m^{-2} for the IC-TLS configuration, see Table 5).

Alone, allometric coefficients were responsible for a large variability for all investigated variables: the range of variation in SA runs (Analysis II) was as large and even sometimes larger than in all simulations from Analyses I and III combined (Table 5). Yet, none of the simulation/configurations accurately represented all features of Wytham woods. All model configurations starting from near bare-ground conditions overestimated GPP, Reco, and NEP, on average by 26%, 30% and 343%, respectively (Table 5). Calibrated model configurations underestimated Reco on average by -19% and hence overestimated NEP by 256%, illustrating the need for optimizing autotrophic and heterotrophic respiration parameters to align those with observational data.

4 Discussion

4.1 The relative weight of the different sources of uncertainty

The different model configurations tested in this study led to very contrasting predictions of vegetation states. Near bare-ground simulations generated potential vegetations that differed in their demography (Figure 4) and land fluxes (Table 5), as a result of the configuration-specific choice of allometries and model structure related to canopy. The finite crown area representation had a substantial impact on the model outputs when using both near bare-ground and prescribed initial conditions. In particular, limiting the crown radius to finite values promoted smaller plants to the detriment of the largest ones (Figure 4), made the simulated LAI closer to the expected value (Table 5), and profoundly modified the vertical distribution of leaves and light in the canopy (Figure 8 and Table 5). Crown size representation appears to drive a large part of the model uncertainty and should be paid more attention to in future analyses of variance decomposition. Especially, because the implementation and the sensitivity of the radiative transfer processes are currently overlooked in ED2.2 like in other vegetation models (Fisher et al. 2018; Viskari et al. 2019). Carbon pools also considerably diverged between model configurations, especially when TLS-derived allometries were taken into account (Table 5). Not surprisingly, leaf and aboveground woody biomass allometries had the largest impact on the corresponding carbon pools (Figure 5).

4.2 The added value of TLS for vegetation modelling

The quantitative information that remote sensing generates at unprecedented spatial and temporal scales can serve to reduce uncertainties in TBM projections. It has already been shown that airborne laser scanning (ALS) combined with an individual-based forest model could offer new insights into the contribution of plant size to ecosystem functioning (Fischer et al. 2019). Similarly, ALS and synthetic-aperture Radar have also successfully been applied to prescribe the initial structure

and composition of tropical forests (Antonarakis et al. 2011; Antonarakis et al. Moorcroft 2014; Longo et al. 2020). Yet, our study illustrates the first attempt to couple TLS and TBMs. As compared to ALS, TLS offers a few significant advantages, as well as some drawbacks, that are important to remember. Airborne techniques allow for wall-to-wall coverage characterizing 3D forest structure at regional scale, whereas TLS offers far more detailed information but only at the local (up to a few ha) scale. Yet, TLS is capable of estimating the volume of individual trees directy, instead of relying on allometric equations that require calibration and thus field measurements. In addition, it can accurately capture the entire size distribution (DBH and height) of the sample plot while smaller trees can easily be missed with airborne surveys (Wang et al. 2016) leading to incorrect demography, especially in dense forests.

Because TLS data are complementary to the datasets that are frequently used for model calibration (e.g. eddy covariance data), they can participate in a collective effort towards realistic representations of ecosystems in TBMs. TLS has the potential to fill important data and process gaps and doing so, to help reduce the uncertainties in vegetation model simulations. The steep increase in the amount of available forest TLS data over the past decade (Calders et al. 2020) makes its coupling with TBMs even more timely. As demonstrated in this study, TLS observation can ensure a more adequate model structure, constrain model allometric parameters and prescribe representative initial conditions.

4.3 Model equifinality

Even though we limited our analysis to a single PFT, hundreds of plant traits can still be calibrated in a vegetation model like ED2.2. Therefore, it is not surprising that multiple sets of parameters can lead to equifinal states. Yet, it is striking to see how critical parameters like SLA and V_{cmax} can end up being so different after calibration when the crown representation or default model allometries changed. All configurations prescribed with initial conditions could accurately simulate the seasonal cycle of GPP observed by the flux tower after calibration (Figure 6). However, those 'optimal' vegetation states were very different from the forest structure point of view (Table 5, Figure 8). This situation perfectly illustrates the low identifiability of numerous TBM parameters and the need for multiple simultaneous constraints and observations. While aboveground carbon storage is critical to estimate forest sink strength and the overall carbon storage capacity of the ecosystem (Keeling and Phillips 2007), it has a limited impact on simulated land fluxes (GPP in particular) that are often used to calibrate TBMs. The parameters controlling land fluxes, namely those controlling ecosystem LAI (Williams and Torn 2015; Wei et al. 2013) and those related to photosynthesis, are highly confounded, echoing observed trade-offs of the Leaf Economic Spectrum (Wright et al. 2004; Peaucelle et al. 2019). TLS has the potential to discriminate equifinal model simulations with similar land fluxes but contrasting structure. On-site trait measurements (Figure 7) could further help avoid those risks of equifinality (Babst et al. 2020; Peaucelle et al. 2019).

4.4 Study limitations

As for any study, the present one has limitations. First, the eddy covariance flux data (2007-2009) preceded the observation of the forest structure (TLS and field inventory occurred in 2015-2016) by almost a decade, which reduces the confidence of

the posterior distributions resulting from the calibration. This is even more true as one realizes that the calibration dataset is rather limited in size and information content (two very similar seasonal cycles of GPP). Yet, here we were more interested in the differences of posterior distributions than their actual shapes. In addition, an imperfect match between different sources of data and/or the low availability of good-quality data are cruel situations that faced any vegetation modeller at least once. We dare to say that as of today, it remains more the rule than the exception, despite very valuable initiatives to standardize high quality data such as Fluxnet (Baldocchi et al. 2001)). Second, the comparison between the potential vegetations as simulated by ED2.2 and the field inventory data are also imperfect as Wytham Woods is a managed forest that has been frequently coppiced and pollarded. Without a better knowledge of the disturbance history experienced by the ecosystem (which is mostly unknown), a perfect reproduction of the current forest demography by the model would only be obtained by compensation processes. Finally, the actual forest composition complexity was completely neglected in this study: we only simulated one PFT while several tree, shrub, and grass species coexist in Wytham Woods. However, integrating this ecological complexity could only have decreased the parameter identifiability while increasing the methodological complexity of this study.

5 Conclusion

Vegetation models are important but are too often used as blackbox tools due to their complexity. They have been intrinsically designed to realistically and accurately represent the ecosystem that they simulate, but often fail to do so primarily because of considerable parameter uncertainties as well as process and initialization errors. Even for the state-of-the-art process-based terrestrial biosphere models, not all parameters can be constrained with data: some cannot be observed in the field, require calibration, or the appropriate observational trait data may be missing. Model calibration can simultaneously lead to satisfactory runs from a fitness perspective while giving unrealistic optimal parameter sets. In addition, model initialization and the choice of model structure necessarily leads to additional uncertainties. We demonstrate in this study that TLS has the potential to provide initial condition estimates and to constrain some critical vegetation model parameters (allometries) and processes (crown representation). Hence, TLS data can help reduce the initialization, model structure and parameter uncertainties. By informing TBMs, TLS can help discriminate realistic states from 'right for the wrong reasons' equifinal vegetation model states.

References

Albani, Marco, David Medvigy, George C. Hurtt, and Paul R. Moorcroft. 2006. "The Contributions of Land-Use Change, CO2 Fertilization, and Climate Variability to the Eastern US Carbon Sink." *Global Change Biology* 12 (12): 2370–90. https://doi.org/10.1111/j.1365-2486.2006.01254.x.

Antonarakis, A. S., J. W. Munger, and P. R. Moorcroft. 2014. "Imaging Spectroscopy- and Lidar-Derived Estimates of Canopy Composition and Structure to Improve Predictions of Forest Carbon Fluxes and Ecosystem Dynamics." *Geophysical Research Letters* 41 (7): 2535–42. https://doi.org/10.1002/2013GL058373.

Antonarakis, A., S. Saatchi, R. Chazdon, and P. Moorcroft. 2011. "Using Lidar and Radar Measurements to Constrain Predictions of Forest Ecosystem Structure and Function." *Ecological Applications : A Publication of the Ecological Society of America*. https://doi.org/10.1890/10-0274.1.

Asner, Gregory P., Roberta E. Martin, Christopher B. Anderson, Katherine Kryston, Nicholas Vaughn, David E. Knapp, Lisa Patrick Bentley, et al. 2017. "Scale Dependence of Canopy Trait Distributions along a Tropical Forest Elevation Gradient." *New Phytologist* 214 (3): 973–88. https://doi.org/10.1111/nph.14068.

Atkin, Owen K., Keith J. Bloomfield, Peter B. Reich, Mark G. Tjoelker, Gregory P. Asner, Damien Bonal, Gerhard Bönisch, et al. 2015. "Global Variability in Leaf Respiration in Relation to Climate, Plant Functional Types and Leaf Traits." *New Phytologist* 206 (2): 614–36. https://doi.org/10.1111/nph.13253.

Babst, Flurin, Andrew D. Friend, Maria Karamihalaki, Jingshu Wei, Georg von Arx, Dario Papale, and Richard L. Peters. 2020. "Modeling Ambitions Outpace Observations of Forest Carbon Allocation." *Trends in Plant Science* 0 (0). https://doi.org/10.1016/j.tplants.2020.10.002.

Baldocchi, Dennis, Eva Falge, Lianhong Gu, Richard Olson, David Hollinger, Steve Running, Peter Anthoni, et al. 2001. "FLUXNET: A New Tool to Study the Temporal and Spatial Variability of Ecosystem-Scale Carbon Dioxide, Water Vapor, and Energy Flux Densities." *Bulletin of the American Meteorological Society* 82 (11): 2415–34. https://doi.org/10.1175/1520-0477(2001)082<2415:FANTTS>2.3.CO;2.

Bonan, Gordon. 2019. *Climate Change and Terrestrial Ecosystem Modeling*. 1st ed. Cambridge University Press. https://doi.org/10.1017/9781107339217.

Bonan, Gordon B. 2008. "Forests and Climate Change: Forcings, Feedbacks, and the Climate Benefits of Forests." *Science* 320 (5882): 1444–49.

Breugel, Michiel van, Johannes Ransijn, Dylan Craven, Frans Bongers, and Jefferson S. Hall. 2011. "Estimating Carbon Stock in Secondary Forests: Decisions and Uncertainties Associated with Allometric Biomass Models." *Forest Ecology and Management* 262 (8): 1648–57. https://doi.org/10.1016/j.foreco.2011.07.018.

Burrascano, S., R. Copiz, E. Del Vico, S. Fagiani, E. Giarrizzo, M. Mei, A. Mortelliti, F. M. Sabatini, and C. Blasi. 2015. "Wild Boar Rooting Intensity Determines Shifts in Understorey Composition and Functional Traits." *Community Ecology* 16 (2): 244–53. https://doi.org/10.1556/168.2015.16.2.12.

Burt, Andrew, Mathias Disney, and Kim Calders. 2019. "Extracting Individual Trees from Lidar Point Clouds Using Treeseg." *Methods in Ecology and Evolution* 10 (3): 438–45. https://doi.org/10.1111/2041-210X.13121.

Butt, Nathalie, Gordon Campbell, Yadvinder Malhi, Mike Morecroft, Katie Fenn, and Matt Thomas. 2009. "Initial Results from Establishment of a Long-Term Broadleaf Monitoring Plot at Wytham Woods, Oxford, UK," January.

Calders, Kim, Jennifer Adams, John Armston, Harm Bartholomeus, Sebastien Bauwens, Lisa Patrick Bentley, Jerome Chave, et al. 2020. "Terrestrial Laser Scanning in Forest Ecology: Expanding the Horizon." *Remote Sensing of Environment* 251 (December): 112102. https://doi.org/10.1016/j.rse.2020.112102.

Calders, Kim, John Armston, Glenn Newnham, Martin Herold, and Nicholas Goodwin. 2014. "Implications of Sensor Configuration and Topography on Vertical Plant Profiles Derived from Terrestrial LiDAR." *Agricultural and Forest Meteorology* 194 (August): 104–17. https://doi.org/10.1016/j.agrformet.2014.03.022.

Calders, Kim, Glenn Newnham, Andrew Burt, Simon Murphy, Pasi Raumonen, Martin Herold, Darius Culvenor, et al. 2015. "Nondestructive Estimates of Above-Ground Biomass Using Terrestrial Laser Scanning." *Methods in Ecology and Evolution* 6 (2): 198–208. https://doi.org/10.1111/2041-210X.12301.

Calders, Kim, Niall Origo, Andrew Burt, Mathias Disney, Joanne Nightingale, Pasi Raumonen, Markku Åkerblom, Yadvinder Malhi, and Philip Lewis. 2018. "Realistic Forest Stand Reconstruction from Terrestrial LiDAR for Radiative Transfer Modelling." *Remote Sensing* 10 (6): 933. https://doi.org/10.3390/rs10060933.

Calders, Kim, Niall Origo, Mathias Disney, Joanne Nightingale, William Woodgate, John Armston, and Philip Lewis. 2018. "Variability and Bias in Active and Passive Ground-Based Measurements of Effective Plant, Wood and Leaf Area Index." *Agricultural and Forest Meteorology* 252 (April): 231–40. https://doi.org/10.1016/j.agrformet.2018.01.029.

Camino, Carlos, Victoria Gonzalez-Dugo, Pilar Hernandez, and Pablo J. Zarco-Tejada. 2019. "Radiative Transfer Vcmax Estimation from Hyperspectral Imagery and SIF Retrievals to Assess Photosynthetic Performance in Rainfed and Irrigated Plant Phenotyping Trials." *Remote Sensing of Environment* 231 (September): 111186. https://doi.org/10.1016/j.rse.2019.05.005.

Cano, Isabel Martínez, Elena Shevliakova, Sergey Malyshev, S. Joseph Wright, Matteo Detto, Stephen W. Pacala, and Helene C. Muller-Landau. 2020. "Allometric Constraints and Competition Enable the Simulation of Size Structure and Carbon Fluxes in a Dynamic Vegetation Model of Tropical Forests (LM3PPA-TV)." *Global Change Biology* 26 (8): 4478–94. https://doi.org/10.1111/gcb.15188.

Chave, J??r??me, Maxime R??jou-M??chain, Alberto B??rquez, Emmanuel Chidumayo, Matthew S. Colgan, Welington B C Delitti, Alvaro Duque, et al. 2014. "Improved Allometric Models to Estimate the Aboveground Biomass of Tropical Trees." *Global Change Biology* 20 (10): 3177–90. https://doi.org/10.1111/gcb.12629.

Collalti, A., S. Marconi, A. Ibrom, C. Trotta, A. Anav, E. D'Andrea, G. Matteucci, et al. 2016. "Validation of 3D-CMCC Forest Ecosystem Model (v.5.1) against Eddy Covariance Data for 10 European Forest Sites." *Geoscientific Model Development* 9 (2): 479–504. https://doi.org/10.5194/gmd-9-479-2016.

Collalti, Alessio, Peter E. Thornton, Alessandro Cescatti, Angelo Rita, Marco Borghetti, Angelo Nolè, Carlo Trotta, Philippe Ciais, and Giorgio Matteucci. 2019. "The Sensitivity of the Forest Carbon Budget Shifts across Processes along with Stand Development and Climate Change." *Ecological Applications* 29 (2): e01837. https://doi.org/10.1002/eap.1837.

Coomes, David A, Steven Heathcote, Elinor R Godfrey, James J Shepherd, and Lawren Sack. 2008. "Scaling of Xylem Vessels and Veins within the Leaves of Oak Species." *Biology Letters* 4 (3): 302–6. https://doi.org/10.1098/rsbl.2008.0094.

Cornelissen, J. H. C. 1996. "An Experimental Comparison of Leaf Decomposition Rates in a Wide Range of Temperate Plant Species and Types." *Journal of Ecology* 84 (4): 573–82. https://doi.org/10.2307/2261479.

Cornelissen, J. H. C., B. Cerabolini, P. Castro-Díez, P. Villar-Salvador, G. Montserrat-Martí, J. P. Puyravaud, M. Maestro, M. J. A. Werger, and R. Aerts. 2003. "Functional Traits of Woody Plants: Correspondence of Species Rankings between Field Adults and Laboratory-Grown Seedlings?" *Journal of Vegetation Science* 14 (3): 311–22. https://doi.org/10.1111/j.1654-1103.2003.tb02157.x.

Cornelissen, Jhc, Pc Diez, and R Hunt. 1996. "Seedling Growth, Allocation and Leaf Attributes in a Wide Range of Woody Plant Species and Types." *Journal of Ecology* 84 (5): 755–65. https://doi.org/10.2307/2261337.

Cornwell, William K., Johannes H. C. Cornelissen, Kathryn Amatangelo, Ellen Dorrepaal, Valerie T. Eviner, Oscar Godoy, Sarah E. Hobbie, et al. 2008. "Plant Species Traits Are the Predominant Control on Litter Decomposition Rates within Biomes Worldwide." *Ecology Letters* 11 (10): 1065–71. https://doi.org/10.1111/j.1461-0248.2008.01219.x.

Diaz, S., J. G. Hodgson, K. Thompson, M. Cabido, J. H. C. Cornelissen, A. Jalili, G. Montserrat-Martí, et al. 2004. "The Plant Traits That Drive Ecosystems: Evidence from Three Continents." *Journal of Vegetation Science* 15 (3): 295–304. https://doi.org/10.1111/j.1654-1103.2004.tb02266.x.

Dietze, Michael C., Shawn P. Serbin, Carl Davidson, Ankur R. Desai, Xiaohui Feng, Ryan Kelly, Rob Kooper, et al. 2014. "A Quantitative Assessment of a Terrestrial Biosphere Model's Data Needs across North American Biomes." *Journal of Geophysical Research: Biogeosciences* 119 (3): 286–300. https://doi.org/10.1002/2013JG002392.

Dietze, Michael C., Michael S. Wolosin, and James S. Clark. 2008. "Capturing Diversity and Interspecific Variability in Allometries: A Hierarchical Approach." *Forest Ecology and Management* 256 (11): 1939–48. https://doi.org/10.1016/j.foreco.2008.07.034.

Ehbrecht, Martin, Peter Schall, Christian Ammer, and Dominik Seidel. 2017. "Quantifying Stand Structural Complexity and Its Relationship with Forest Management, Tree Species Diversity and Microclimate." *Agricultural and Forest Meteorology* 242 (August): 1–9. https://doi.org/10.1016/j.agrformet.2017.04.012.

Elzhov, Timur V., Katharine M. Mullen, Andrej-Nikolai Spiess, and Ben Bolker. 2016. *Minpack.Lm: R Interface to the Levenberg-Marquardt Nonlinear Least-Squares Algorithm Found in MINPACK, Plus Support for Bounds* (version 1.2-1). https://CRAN.R-project.org/package=minpack.lm.

Esprey, L. J, P. J Sands, and C. W Smith. 2004. “Understanding 3-PG Using a Sensitivity Analysis.” *Forest Ecology and Management*, Synthesis of the physiological, environmental, genetic and silvicultural determinants of the growth and productivity of eucalypts in plantations., 193 (1): 235–50. https://doi.org/10.1016/j.foreco.2004.01.032.

Falster, Daniel S., Remko A. Duursma, Masae I. Ishihara, Diego R. Barneche, Richard G. FitzJohn, Angelica Vårhammar, Masahiro Aiba, et al. 2015. “BAAD: A Biomass And Allometry Database for Woody Plants.” *Ecology* 96 (5): 1445–1445. https://doi.org/10.1890/14-1889.1.

Fan, Guangpeng, Liangliang Nan, Yanqi Dong, Xiaohui Su, and Feixiang Chen. 2020. “AdQSM: A New Method for Estimating Above-Ground Biomass from TLS Point Clouds.” *Remote Sensing* 12 (18): 3089. https://doi.org/10.3390/rs12183089.

Fenn, K., Y. Malhi, M. Morecroft, C. Lloyd, and M. Thomas. 2015. “The Carbon Cycle of a Maritime Ancient Temperate Broadleaved Woodland at Seasonal and Annual Scales.” *Ecosystems* 18 (1): 1–15. https://doi.org/10.1007/s10021-014-9793-1.

Fer, Istem, Ryan Kelly, Paul R. Moorcroft, Andrew D. Richardson, Elizabeth M. Cowdery, and Michael C. Dietze. 2018. “Linking Big Models to Big Data: Efficient Ecosystem Model Calibration through Bayesian Model Emulation.” *Biogeosciences* 15 (19): 5801–30. https://doi.org/10.5194/bg-15-5801-2018.

Fischer, Fabian Jörg, Isabelle Maréchaux, and Jérôme Chave. 2019. “Improving Plant Allometry by Fusing Forest Models and Remote Sensing.” *New Phytologist* 223 (3): 1159–65. https://doi.org/10.1111/nph.15810.

Fisher, Rosie A., Charles D. Koven, William R. L. Anderegg, Bradley O. Christoffersen, Michael C. Dietze, Caroline E. Farrior, Jennifer A. Holm, et al. 2018. “Vegetation Demographics in Earth System Models: A Review of Progress and Priorities.” *Global Change Biology* 24 (1): 35–54. https://doi.org/10.1111/gcb.13910.

Friedlingstein, P., P. Cox, R. Betts, L. Bopp, W. von Bloh, V. Brovkin, P. Cadule, et al. 2006. “Climate–Carbon Cycle Feedback Analysis: Results from the C4MIP Model Intercomparison.” *Journal of Climate* 19 (14): 3337–53. https://doi.org/10.1175/JCLI3800.1.

Friedlingstein, Pierre, Malte Meinshausen, Vivek K. Arora, Chris D. Jones, Alessandro Anav, Spencer K. Liddicoat, and Reto Knutti. 2014. “Uncertainties in CMIP5 Climate Projections Due to Carbon Cycle Feedbacks.” *Journal of Climate* 27 (2): 511–26. https://doi.org/10.1175/JCLI-D-12-00579.1.

Garnier, Eric, Sandra Lavorel, Pauline Ansquer, Helena Castro, Pablo Cruz, Jiri Dolezal, Ove Eriksson, et al. 2007. “Assessing the Effects of Land-Use Change on Plant Traits, Communities and Ecosystem Functioning in Grasslands: A Standardized Methodology and Lessons from an Application to 11 European Sites.” *Annals of Botany* 99 (5): 967–85. https://doi.org/10.1093/aob/mcl215.

Giarrizzo, Eleonora, Sabina Burrascano, Tommaso Chiti, Francesco de Bello, Jan Lepš, Laura Zavattero, and Carlo Blasi. 2017. “Re-visiting Historical Semi-natural Grasslands in the Apennines to Assess Patterns of Changes in Species Composition and Functional Traits.” https://pubag.nal.usda.gov/catalog/5879480.

Hackenberg, Jan, Heinrich Spiecker, Kim Calders, Mathias Disney, and Pasi Raumonen. 2015. “SimpleTree —An Efficient Open Source Tool to Build Tree Models from TLS Clouds.” *Forests* 6 (11): 4245–94. https://doi.org/10.3390/f6114245.

Hall, Jeanette, Keith Kirby, and A Whitbread. 2001. *National Vegetation Classification: Field Guide to Woodland*.

Hopkinson, Chris, Laura Chasmer, Colin Young-Pow, and Paul Treitz. 2011. “Assessing Forest Metrics with a Ground-Based Scanning Lidar.” *Canadian Journal of Forest Research*, February. https://doi.org/10.1139/x03-225.

Hurtt, G. C., J. Fisk, R. Q. Thomas, R. Dubayah, P. R. Moorcroft, and H. H. Shugart. 2010. “Linking Models and Data on Vegetation Structure.” *Journal of Geophysical Research: Biogeosciences* 115 (G2). https://doi.org/10.1029/2009JG000937.

Jones, Hamlyn G., and Robin A. Vaughan. 2010. *Remote Sensing of Vegetation: Principles, Techniques, and Applications*. OUP Oxford.

Jupp, David L. B., D. S. Culvenor, J. L. Lovell, G. J. Newnham, A. H. Strahler, and C. E. Woodcock. 2009. “Estimating Forest LAI Profiles and Structural Parameters Using a Ground-Based Laser Called ‘Echidna®.” *Tree Physiology* 29 (2): 171–81. https://doi.org/10.1093/treephys/tpn022.

Kattge, Jens, Gerhard Bönisch, Sandra Díaz, Sandra Lavorel, Iain Colin Prentice, Paul Leadley, Susanne Tautenhahn, et al. 2020. “TRY Plant Trait Database – Enhanced Coverage and Open Access.” *Global Change Biology* 26 (1): 119–88. https://doi.org/10.1111/gcb.14904.

Kattge, Jens, Wolfgang Knorr, Thomas Raddatz, and Christian Wirth. 2009. "Quantifying Photosynthetic Capacity and Its Relationship to Leaf Nitrogen Content for Global-Scale Terrestrial Biosphere Models." *Global Change Biology* 15 (4): 976–91. https://doi.org/10.1111/j.1365-2486.2008.01744.x.

Keeling, Helen C., and Oliver L. Phillips. 2007. "The Global Relationship between Forest Productivity and Biomass." *Global Ecology and Biogeography* 16 (5): 618–31. https://doi.org/10.1111/j.1466-8238.2007.00314.x.

Kleyer, M., R. M. Bekker, I. C. Knevel, J. P. Bakker, K. Thompson, M. Sonnenschein, P. Poschlod, et al. 2008. "The LEDA Traitbase: A Database of Life-History Traits of the Northwest European Flora." *Journal of Ecology* 96 (6): 1266–74. https://doi.org/10.1111/j.1365-2745.2008.01430.x.

LeBauer, David S., Dan Wang, Katherine T. Richter, Carl C. Davidson, and Michael C. Dietze. 2013. "Facilitating Feedbacks between Field Measurements and Ecosystem Models." *Ecological Monographs* 83 (2): 133–54.

Liebergesell, Mario, Björn Reu, Ulrike Stahl, Martin Freiberg, Erik Welk, Jens Kattge, J. Hans C. Cornelissen, Josep Peñuelas, and Christian Wirth. 2016. "Functional Resilience against Climate-Driven Extinctions – Comparing the Functional Diversity of European and North American Tree Floras." *PLOS ONE* 11 (2): e0148607. https://doi.org/10.1371/journal.pone.0148607.

Lin, J. C., M. R. Pejam, E. Chan, S. C. Wofsy, E. W. Gottlieb, H. A. Margolis, and J. H. McCaughey. 2011. "Attributing Uncertainties in Simulated Biospheric Carbon Fluxes to Different Error Sources." *Global Biogeochemical Cycles* 25 (2). https://doi.org/10.1029/2010GB003884.

Longo, Marcos, Ryan G. Knox, David M. Medvigy, Naomi M. Levine, Michael C. Dietze, Yeonjoo Kim, Abigail L. S. Swann, et al. 2019. "The Biophysics, Ecology, and Biogeochemistry of Functionally Diverse, Vertically and Horizontally Heterogeneous Ecosystems: The Ecosystem Demography Model, Version 2.2 – Part 1: Model Description." *Geoscientific Model Development* 12 (10): 4309–46. https://doi.org/10.5194/gmd-12-4309-2019.

Longo, Marcos, Sassan Saatchi, Michael Keller, Kevin Bowman, António Ferraz, Paul R. Moorcroft, Douglas C. Morton, et al. 2020. "Impacts of Degradation on Water, Energy, and Carbon Cycling of the Amazon Tropical Forests." *Journal of Geophysical Research: Biogeosciences* 125 (8): e2020JG005677. https://doi.org/10.1029/2020JG005677.

Lovell, J. L., D. L. B. Jupp, D. S. Culvenor, and N. C. Coops. 2003. "Using Airborne and Ground-Based Ranging Lidar to Measure Canopy Structure in Australian Forests." *Canadian Journal of Remote Sensing* 29 (5): 607–22. https://doi.org/10.5589/m03-026.

Lovenduski, Nicole S., and Gordon B. Bonan. 2017. "Reducing Uncertainty in Projections of Terrestrial Carbon Uptake." *Environmental Research Letters* 12 (4): 044020. https://doi.org/10.1088/1748-9326/aa66b8.

Luo, Yiqi, Ensheng Weng, Xiaowen Wu, Chao Gao, Xuhui Zhou, and Li Zhang. 2009. "Parameter Identifiability, Constraint, and Equifinality in Data Assimilation with Ecosystem Models." *Ecological Applications* 19 (3): 571–74. https://doi.org/10.1890/08-0561.1.

Maas, H.-G., A. Bienert, S. Scheller, and E. Keane. 2008. "Automatic Forest Inventory Parameter Determination from Terrestrial Laser Scanner Data." *International Journal of Remote Sensing* 29 (5): 1579–93. https://doi.org/10.1080/01431160701736406.

Maire, Vincent, Ian J. Wright, I. Colin Prentice, Niels H. Batjes, Radika Bhaskar, Peter M. van Bodegom, Will K. Cornwell, et al. 2015. "Global Effects of Soil and Climate on Leaf Photosynthetic Traits and Rates." *Global Ecology and Biogeography* 24 (6): 706–17. https://doi.org/10.1111/geb.12296.

Massoud, Elias C., Chonggang Xu, Rosie A. Fisher, Ryan G. Knox, Anthony P. Walker, Shawn P. Serbin, Bradley O. Christoffersen, et al. 2019. "Identification of Key Parameters Controlling Demographically Structured Vegetation Dynamics in a Land Surface Model: CLM4.5(FATES)." *Geoscientific Model Development* 12 (9): 4133–64. https://doi.org/10.5194/gmd-12-4133-2019.

McGuire, A. D., S. Sitch, J. S. Clein, R. Dargaville, G. Esser, J. Foley, M. Heimann, et al. 2001. "Carbon Balance of the Terrestrial Biosphere in the Twentieth Century: Analyses of CO2, Climate and Land Use Effects with Four Process-Based Ecosystem Models." *Global Biogeochemical Cycles* 15 (1): 183–206. https://doi.org/10.1029/2000GB001298.

Medlyn, B. E., F.-W. Badeck, D. G. G. De Pury, C. V. M. Barton, M. Broadmeadow, R. Ceulemans, P. De Angelis, et al. 1999. "Effects of Elevated [CO2] on Photosynthesis in European Forest Species: A Meta-Analysis of Model Parameters." *Plant, Cell & Environment* 22 (12): 1475–95. https://doi.org/10.1046/j.1365-3040.1999.00523.x.

Medvigy, D., S. C. Wofsy, J. W. Munger, D. Y. Hollinger, and P. R. Moorcroft. 2009. "Mechanistic Scaling of Ecosystem Function and Dynamics in Space and Time: Ecosystem Demography Model Version 2." *Journal of Geophysical Research: Biogeosciences* 114 (G1). https://doi.org/10.1029/2008JG000812.

Medvigy, David, and Paul R. Moorcroft. 2012. "Predicting Ecosystem Dynamics at Regional Scales: An Evaluation of a Terrestrial Biosphere Model for the Forests of Northeastern North America." *Philosophical Transactions of the Royal Society of London B: Biological Sciences* 367 (1586): 222–35. https://doi.org/10.1098/rstb.2011.0253.

Milla, Rubén, and Peter B. Reich. 2011. "Multi-Trait Interactions, Not Phylogeny, Fine-Tune Leaf Size Reduction with Increasing Altitude." *Annals of Botany* 107 (3): 455–65. https://doi.org/10.1093/aob/mcq261.

Moorcroft, Paul R., G. C. Hurtt, and Stephen W. Pacala. 2001. "A Method for Scaling Vegetation Dynamics: The Ecosystem Demography Model (ED)." *Ecological Monographs* 71 (4): 557–86.

Niinemets, Ülo. 2001. "Global-Scale Climatic Controls of Leaf Dry Mass Per Area, Density, and Thickness in Trees and Shrubs." *Ecology* 82 (2): 453–69. https://doi.org/10.1890/0012-9658(2001)082[0453:GSCCOL]2.0.CO;2.

Ogaya, R., and J. Peñuelas. 2003. "Comparative Field Study of Quercus Ilex and Phillyrea Latifolia: Photosynthetic Response to Experimental Drought Conditions." https://doi.org/10.1016/S0098-8472(03)00019-4.

Ordoñez, Jenny C., Peter M. van Bodegom, Jan-Philip M. Witte, Ruud P. Bartholomeus, Jurgen R. van Hal, and Rien Aerts. 2010. "Plant Strategies in Relation to Resource Supply in Mesic to Wet Environments: Does Theory Mirror Nature?" *The American Naturalist* 175 (2): 225–39. https://doi.org/10.1086/649582.

Paine, C. E. Timothy, Lucy Amissah, Harald Auge, Christopher Baraloto, Martin Baruffol, Nils Bourland, Helge Bruelheide, et al. 2015. "Globally, Functional Traits Are Weak Predictors of Juvenile Tree Growth, and We Do Not Know Why." *Journal of Ecology* 103 (4): 978–89. https://doi.org/10.1111/1365-2745.12401.

Peaucelle, Marc, Cédric Bacour, Philippe Ciais, Nicolas Vuichard, Sylvain Kuppel, Josep Peñuelas, Luca Belelli Marchesini, et al. 2019. "Covariations between Plant Functional Traits Emerge from Constraining Parameterization of a Terrestrial Biosphere Model." *Global Ecology and Biogeography* 28 (9): 1351–65. https://doi.org/10.1111/geb.12937.

Poulter, Benjamin, Fred Hattermann, Ed Hawkins, Sönke Zaehle, Stephen Sitch, Natalia Restrepo-Coupe, Ursula Heyder, and Wolfgang Cramer. 2010. "Robust Dynamics of Amazon Dieback to Climate Change with Perturbed Ecosystem Model Parameters." *Global Change Biology* 16 (9): 2476–95. https://doi.org/10.1111/j.1365-2486.2009.02157.x.

Raczka, Brett, Michael C. Dietze, Shawn P. Serbin, and Kenneth J. Davis. 2018. "What Limits Predictive Certainty of Long-Term Carbon Uptake?" *Journal of Geophysical Research: Biogeosciences* 123 (12): 3570–88. https://doi.org/10.1029/2018JG004504.

Raumonen, Pasi, Mikko Kaasalainen, Markku Åkerblom, Sanna Kaasalainen, Harri Kaartinen, Mikko Vastaranta, Markus Holopainen, Mathias Disney, and Philip Lewis. 2013. "Fast Automatic Precision Tree Models from Terrestrial Laser Scanner Data." *Remote Sensing* 5 (2): 491–520. https://doi.org/10.3390/rs5020491.

Reich, Peter B., Jacek Oleksyn, and Ian J. Wright. 2009. "Leaf Phosphorus Influences the Photosynthesis–Nitrogen Relation: A Cross-Biome Analysis of 314 Species." *Oecologia* 160 (2): 207–12. https://doi.org/10.1007/s00442-009-1291-3.

Rezende, L. C., B. Arenque, C. von Randow, M. S. Moura, S. D. Aidar, M. S. Buckeridge, R. Menezes, L. S. Souza, and J. P. Ometto. 2013. "Calibration of the Maximum Carboxylation Velocity (Vcmax) for the Caatinga for Use in Dynamic Global Vegetation Models (DGVMs)." *AGU Fall Meeting Abstracts* 11 (December): B11A-0366.

Rezende, L. F. C., B. C. Arenque-Musa, M. S. B. Moura, S. T. Aidar, C. Von Randow, R. S. C. Menezes, J. P. B. H. Ometto, et al. 2016. "Calibration of the Maximum Carboxylation Velocity (Vcmax) Using Data Mining Techniques and Ecophysiological Data from the Brazilian Semiarid Region, for Use in Dynamic Global Vegetation Models." *Brazilian Journal of Biology* 76 (2): 341–51. https://doi.org/10.1590/1519-6984.14414.

Richardson, Andrew D., Mathew Williams, David Y. Hollinger, David J. P. Moore, D. Bryan Dail, Eric A. Davidson, Neal A. Scott, et al. 2010. "Estimating Parameters of a Forest Ecosystem C Model with Measurements of Stocks and Fluxes as Joint Constraints." *Oecologia* 164 (1): 25–40.

Roberts, J., R. Hopkins, and M. Morecroft. 1999. "Towards a Predictive Description of Forest Canopies from Litter Properties." *Functional Ecology* 13 (2): 265–72. https://doi.org/10.1046/j.1365-2435.1999.00312.x.

Rogers, Alistair, Belinda E. Medlyn, Jeffrey S. Dukes, Gordon Bonan, Susanne von Caemmerer, Michael C. Dietze, Jens Kattge, et al. 2017. "A Roadmap for Improving the Representation of Photosynthesis in Earth System Models." *New Phytologist* 213 (1): 22–42. https://doi.org/10.1111/nph.14283.

Saarinen, Ninni, Kim Calders, Ville Kankare, Tuomas Yrttimaa, Samuli Junttila, Ville Luoma, Saija Huuskonen, Jari Hynynen, and Hans Verbeeck. n.d. "Understanding 3D Structural Complexity of Individual Scots Pine Trees with Different Management History." *Ecology and Evolution* n/a (n/a). Accessed February 19, 2021. https://doi.org/10.1002/ece3.7216.

Sakschewski, Boris, Werner von Bloh, Alice Boit, Anja Rammig, Jens Kattge, Lourens Poorter, Josep Peñuelas, and Kirsten Thonicke. 2015. "Leaf and Stem Economics Spectra Drive Diversity of Functional Plant Traits in a Dynamic Global Vegetation Model." *Global Change Biology* 21 (7): 2711–25. https://doi.org/10.1111/gcb.12870.

Savill, Peter, Christopher Perrins, Keith Kirby, and Nigel Fisher. 2010. *Wytham Woods: Oxford's Ecological Laboratory*. OUP Oxford.

Scherer-Lorenzen, Michael, Ernst-Detlef Schulze, Axel Don, Jens Schumacher, and Eberhard Weller. 2007. "Exploring the Functional Significance of Forest Diversity: A New Long-Term Experiment with Temperate Tree Species (BIOTREE)." *Perspectives in Plant Ecology, Evolution and Systematics* 9 (2): 53–70. https://doi.org/10.1016/j.ppees.2007.08.002.

Shiklomanov, Alexey N., Ben Bond-Lamberty, Jeff W. Atkins, and Christopher M. Gough. 2020. "Structure and Parameter Uncertainty in Centennial Projections of Forest Community Structure and Carbon Cycling." *Global Change Biology*, August, gcb.15164. https://doi.org/10.1111/gcb.15164.

Shipley, B. 2002. "Trade-Offs between Net Assimilation Rate and Specific Leaf Area in Determining Relative Growth Rate: Relationship with Daily Irradiance." *Functional Ecology* 16 (5): 682–89. https://doi.org/10.1046/j.1365-2435.2002.00672.x.

Stiers, Melissa, Katharina Willim, Dominik Seidel, Martin Ehbrecht, Myroslav Kabal, Christian Ammer, and Peter Annighöfer. 2018. "A Quantitative Comparison of the Structural Complexity of Managed, Lately Unmanaged and Primary European Beech (Fagus Sylvatica L.) Forests." *Forest Ecology and Management* 430 (December): 357–65. https://doi.org/10.1016/j.foreco.2018.08.039.

Takoudjou, Stéphane Momo, Pierre Ploton, Bonaventure Sonké, Jan Hackenberg, Sébastien Griffon, Francois de Coligny, Narcisse Guy Kamdem, et al. 2018. "Using Terrestrial Laser Scanning Data to Estimate Large Tropical Trees Biomass and Calibrate Allometric Models: A Comparison with Traditional Destructive Approach." *Methods in Ecology and Evolution* 9 (4): 905–16. https://doi.org/10.1111/2041-210X.12933.

Tan, Kun, Philippe Ciais, Shilong Piao, Xiaopu Wu, Yanhong Tang, Nicolas Vuichard, Shuang Liang, and Jingyun Fang. 2010. "Application of the ORCHIDEE Global Vegetation Model to Evaluate Biomass and Soil Carbon Stocks of Qinghai-Tibetan Grasslands." *Global Biogeochemical Cycles* 24 (1). https://doi.org/10.1029/2009GB003530.

Tanago, Jose Gonzalez de, Alvaro Lau, Harm Bartholomeus, Martin Herold, Valerio Avitabile, Pasi Raumonen, Christopher Martius, et al. 2018. "Estimation of Above-Ground Biomass of Large Tropical Trees with Terrestrial LiDAR." *Methods in Ecology and Evolution* 9 (2): 223–34. https://doi.org/10.1111/2041-210X.12904.

Thomas, M. V., Y. Malhi, K. M. Fenn, J. B. Fisher, M. D. Morecroft, C. R. Lloyd, M. E. Taylor, and D. D. McNeil. 2011. "Carbon Dioxide Fluxes over an Ancient Broadleaved Deciduous Woodland in Southern England." *Biogeosciences* 8 (6): 1595–1613. https://doi.org/10.5194/bg-8-1595-2011.

Viovy, Nicolas. 2018. "CRUNCEP Version 7 - Atmospheric Forcing Data for the Community Land Model." UCAR/NCAR - Research Data Archive. https://doi.org/10.5065/PZ8F-F017.

Viskari, Toni, Alexey Shiklomanov, Michael C. Dietze, and Shawn P. Serbin. 2019. "The Influence of Canopy Radiation Parameter Uncertainty on Model Projections of Terrestrial Carbon and Energy Cycling." *PLOS ONE* 14 (7): e0216512. https://doi.org/10.1371/journal.pone.0216512.

Wang, Y., J. Hyyppä, X. Liang, H. Kaartinen, X. Yu, E. Lindberg, J. Holmgren, et al. 2016. "International Benchmarking of the Individual Tree Detection Methods for Modeling 3-D Canopy Structure for Silviculture and Forest Ecology Using Airborne Laser Scanning." *IEEE Transactions on Geoscience and Remote Sensing* 54 (9): 5011–27. https://doi.org/10.1109/TGRS.2016.2543225.

Wei, Helin, Youlong Xia, Kenneth E. Mitchell, and Michael B. Ek. 2013. "Improvement of the Noah Land Surface Model for Warm Season Processes: Evaluation of Water and Energy Flux Simulation." *Hydrological Processes* 27 (2): 297–303. https://doi.org/10.1002/hyp.9214.

Williams, Ian N., and Margaret S. Torn. 2015. "Vegetation Controls on Surface Heat Flux Partitioning, and Land-Atmosphere Coupling." *Geophysical Research Letters* 42 (21): 9416–24. https://doi.org/10.1002/2015GL066305.

Wirth, Christian, and Jeremy W. Lichstein. 2009. "The Imprint of Species Turnover on Old-Growth Forest Carbon Balances - Insights From a Trait-Based Model of Forest Dynamics." In *Old-Growth Forests: Function, Fate and Value*, edited by Christian Wirth, Gerd Gleixner, and Martin Heimann, 81–113. Ecological Studies. Berlin, Heidelberg: Springer. https://doi.org/10.1007/978-3-540-92706-8_5.

Wramneby, Anna, Benjamin Smith, Sönke Zaehle, and Martin T. Sykes. 2008. "Parameter Uncertainties in the Modelling of Vegetation Dynamics—Effects on Tree Community Structure and Ecosystem Functioning in European Forest Biomes." *Ecological Modelling* 216 (3): 277–90. https://doi.org/10.1016/j.ecolmodel.2008.04.013.

Wright, Ian J., Peter B. Reich, Mark Westoby, David D. Ackerly, Zdravko Baruch, Frans Bongers, Jeannine Cavender-Bares, et al. 2004. "The Worldwide Leaf Economics Spectrum." *Nature* 428 (6985): 821–27. https://doi.org/10.1038/nature02403.

Zaehle, S., S. Sitch, B. Smith, and F. Hatterman. 2005. "Effects of Parameter Uncertainties on the Modeling of Terrestrial Biosphere Dynamics." *Global Biogeochemical Cycles* 19 (3). https://doi.org/10.1029/2004GB002395.

Code and data availability

The code of the ED2.2 model is ~~available~~ stored as a permanent release at~~on Github at~~ https://github.com/~~EDmodel~~mpaiao/releases/tag/rev-86~~ED2 (tag v.2.2.0)~~. All data and scripts used in this study are also stored on github at ~~(~~https://github.com/femeunier/LidarED~~)~~ (tag v1.0, DOI: 10.5281/zenodo.4664035).~~.~~

Author contribution

F.M., S.M.K.M., M.P., K.C., L.T., W.V. and H.V. designed the study. K.C. collected the TLS data with the help and support from N.O., J.N., and M.D. S.M.K.M. and K.C. formatted the TLS data. F.M. prepared the model, ran the simulations and analyzed the results. F.M. wrote the first version of the manuscript and all co-authors critically revised it. Inventory data were provided by Y.M.

Acknowledgements

This research was funded by BELSPO (Belgian Science Policy Office) in the frame of the STEREO III programme – project 3D-FOREST (SR/02/355). The computational resources and services used in this work were provided by the VSC (Flemish Supercomputer Center), funded by the Research Foundation - Flanders (FWO) and the Flemish Government – department EWI. During the preparation of this manuscript, F.M. was funded by the FWO as a junior postdoc and is thankful to this organization for its financial support. N.S. was funded by the Academy of Finland (project number 315079). K.C was funded by the European Union's Horizon 2020 research and innovation programme under the Marie Sklodowska-Curie grant agreement No 835398. M.P. was funded by the FWO (grant No. G018319N) and the European Union's Horizon 2020 research and innovation programme under the Marie Sklodowska-Curie grant agreement No. 891369. The TLS fieldwork was funded through the Metrology for Earth Observation and Climate project (MetEOC-2), grant number ENV55 within the European Metrology Research Programme (EMRP). The EMRP is jointly funded by the EMRP participating countries within EURAMET and the European Union. Funds for purchase of the UCL RIEGL VZ-400 instrument was provided by the UK NERC National Centre for Earth Observation (NCEO). The census of the forest plot was supported by an ERC Advanced Investigator Grant to Y.M. (GEM-TRAIT, grant number 321131).

Figures and Tables

Tables

Table 1: Mean (± one standard deviation) of traits (Specific Leaf Area or SLA, and maximum rate of carboxylation or V_{cmax}) available in the TRY database for each of the five dominant species in Wytham woods, and their local prevalence (in terms of individual density and basal area). The community weighted means (CWM) and standard deviations (CWSD) were obtained using the basal areas as weights. Missing traits were unavailable in TRY when we consulted it. Total number of inventoried trees = 821, total basal area = 50.71 m² for the 1.4 plot.

Ap = Acer pseudoplatanus, Ca = Corylus avellana, Cm = Crataegus monogyna, Fe = Fraxinus excelsior, and Qr = Quercus robur. The colours of the different species in the first row of the Table are consistent with Figures 1 and 3.

Trait	Ap	Ca	Cm	Fe	Qr	Others	CWM (± CWSD)
SLA ($m^2\ kg_C^{-1}$)	-	34.7 (± 36.1)	62.8 (± 65.5)	-	22.9 (± 23.9)	-	25.1 (± 1.5)
V_{cmax} ($\mu mol\ m^{-2}\ s^{-1}$)	31.9 (± 16.1)	-	-	39.7 (± 18.0)	31.1 (± 18.8)	-	32.6 (± 0.9)
Density (-)	532	67	24	84	35	79	
Basal area (m^2)	31.59	0.48	0.24	5.96	11.87	0.57	

Table 2: List of allometries modified in this study, ED2.2 default and TLS-derived allometric coefficients. DBH = Diameter at Breast Height (cm).

Allometry	Equation	Parameter	Default	TLS
Height, *h* (m)	$h = h_{ref} + h_1 \cdot [1 - exp(DBH \cdot h_2)]$	h_{ref}	1.3	-3.1
		h_1	25.18	26.11
		h_2	-0.050	-0.073
Aboveground woody biomass, B_d (kg)	$B_d = B_{d1} \cdot DBH^{B_{d2}}$	B_{d1}	0.11	0.37
		B_{d2}	2.46	2.29
Crown area, *CA* (m²)	$CA = CA_1 \cdot DBH^{CA_2}$	CA_1	2.49	0.63
		CA_2	0.81	1.14
Leaf biomass, B_l (kg)	$B_l = B_{l1} \cdot DBH^{B_{l2}}$	B_{l1}	0.048	0.081
		B_{l2}	1.46	1.46

Table 3: Model prior distributions, default values, and posterior medians.

Parameter	Prior(a,b)	ED2.2 default	Posterior median		
			IC-Default	IC-FC	IC-TLS
V_{cmax} ($\mu mol\ m^{-2}\ s^{-1}$)	unif(5,60)	17.5	47.3	13.2	16.7
SLA ($m^2\ kg_C^{-1}$)	unif(5,70)	24.2	14.4	39.8	26.9

780

Table 4: Summary of the model configurations used in this study and the underlying model setups.

		Configuration						
		Analysis I			Analysis II	Analysis III		
		NBG-Default	NBG-FC	NBG-TLS	SA	IC-Default	IC-FC	IC-TLS
Process	Initial conditions	Near-bare ground	Near-bare ground	Near-bare ground	Inventory	Inventory	TLS	TLS
	Crown representation	Infinitely wide	Finite radius	Finite radius	Finite radius	Infinitely wide	Finite radius	Finite radius
	Allometric parameters	Default	Default	TLS	Default or TLS	Default	Default	TLS
	Run length (years)	100	100	100	3	3	3	3

Figures

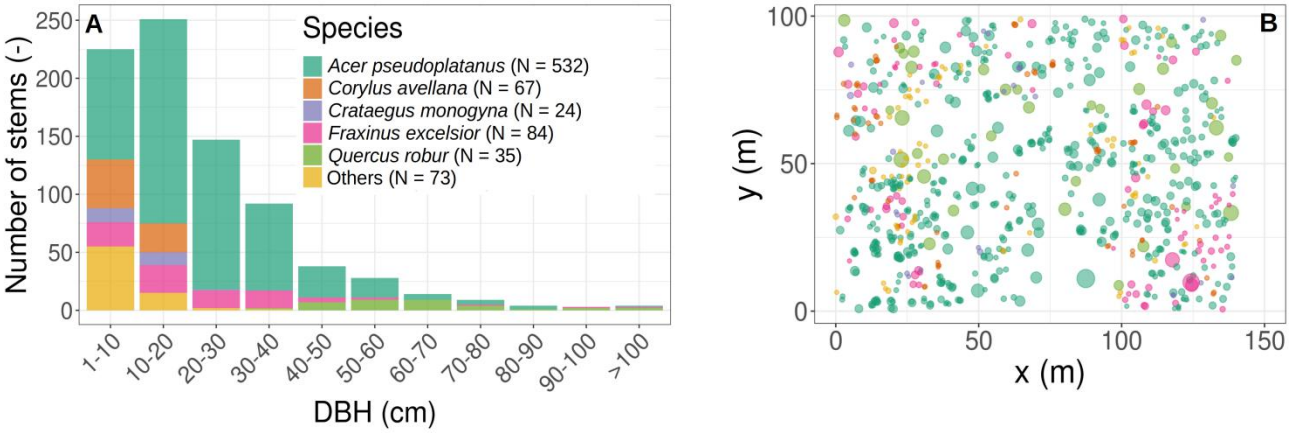

785

Figure 1: Initial conditions in terms of tree size distribution and composition (A), horizontal position, basal area (not to scale), and composition (B). The species colour legend applies to both panels and is kept the same for Figure 3 below. In the simulations, all trees were classified into a single plant functional type (Mid-successional temperate deciduous).

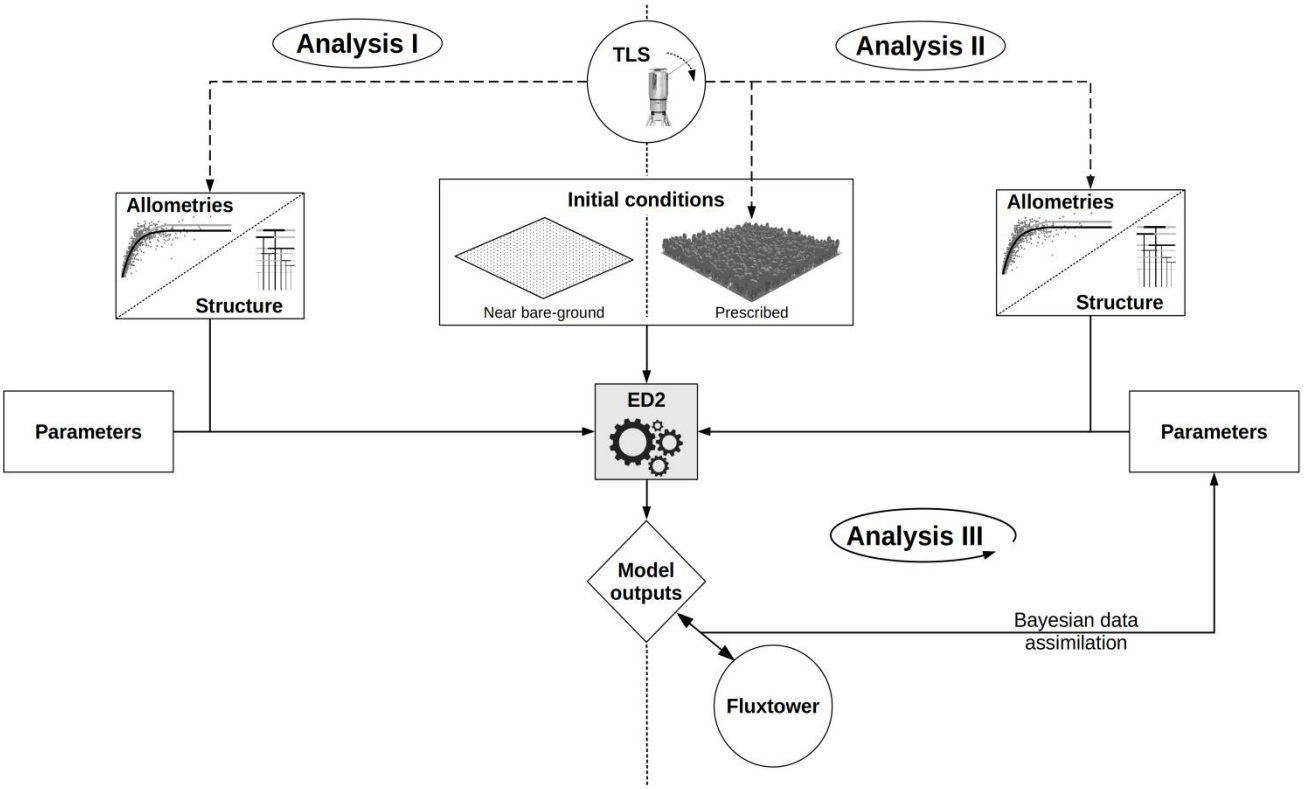

Figure 2: Schematic workflow of this study. Terrestrial LiDAR scanning (TLS) data were used to feed the Ecosystem Demography model, version 2.2 (ED2.2), and impose model allometric equations, vegetation structure and initial conditions. The study was separated into three main analyses that aim to assess the impact of vegetation structure, as derived from TLS data, on model outputs. More specifically, simulated potential vegetations (Analysis I), short-term forest functioning (Analysis II), and model calibration (Analysis III) were each time compared between simulations that were informed by TLS data and simulations run with default model configuration.

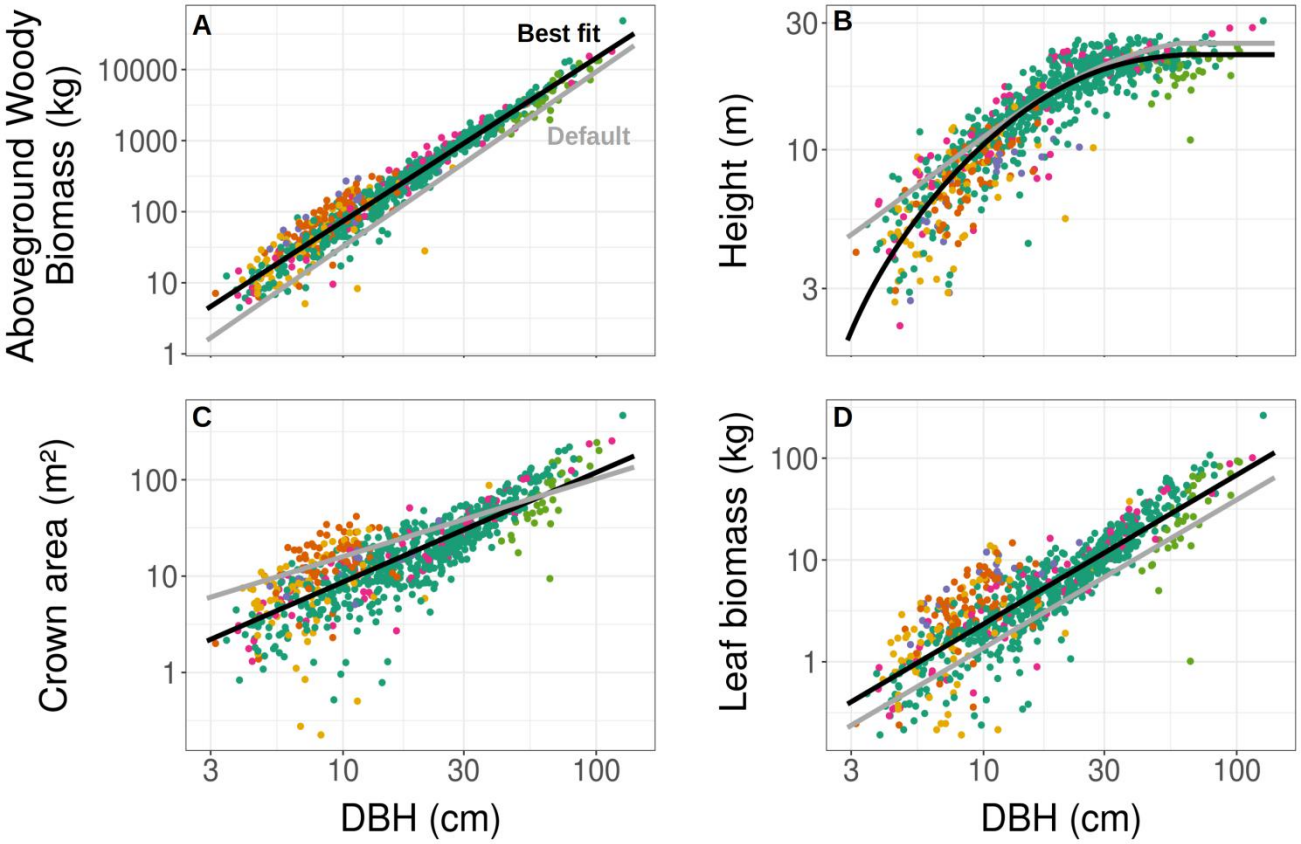

800 **Figure 3: TLS-derived (black) and default (grey) model allometries for the aboveground woody biomass (A), tree height (B), crown area (C), and leaf biomass (D). The data to which the TLS allometries were fitted (coloured points corresponding to the tree species detailed in Figure 1) were obtained using TLS.**

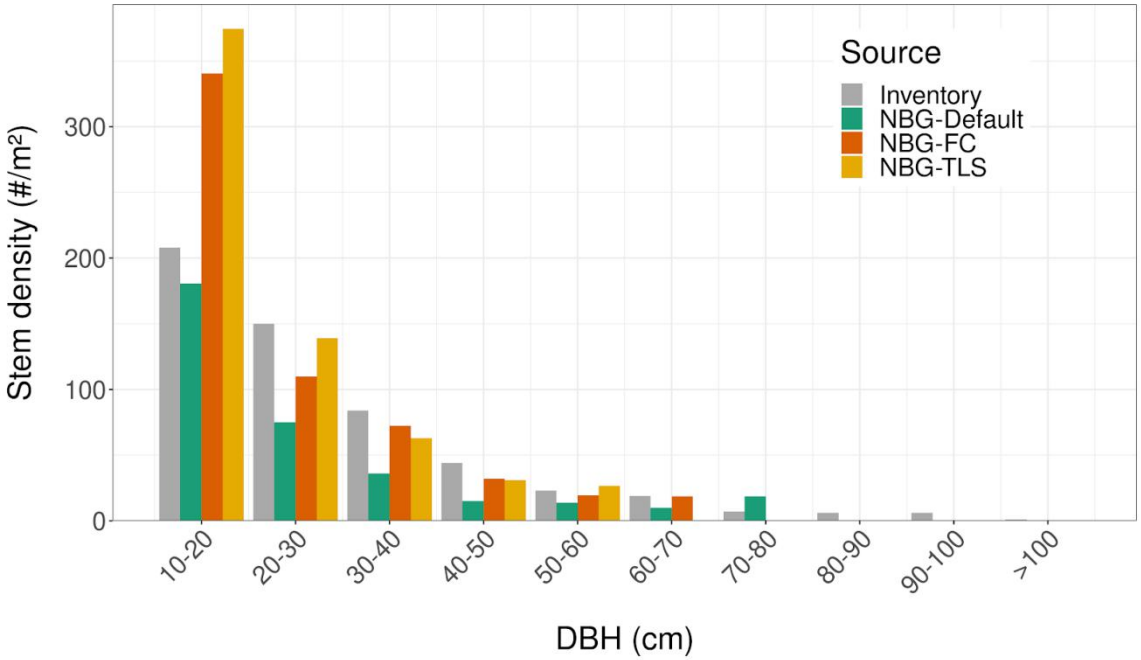

Figure 4: Size distribution of the three configurations starting from near bare-ground initial conditions after 100 years of simulations (Analysis I), and how they compare to the field inventory (grey).

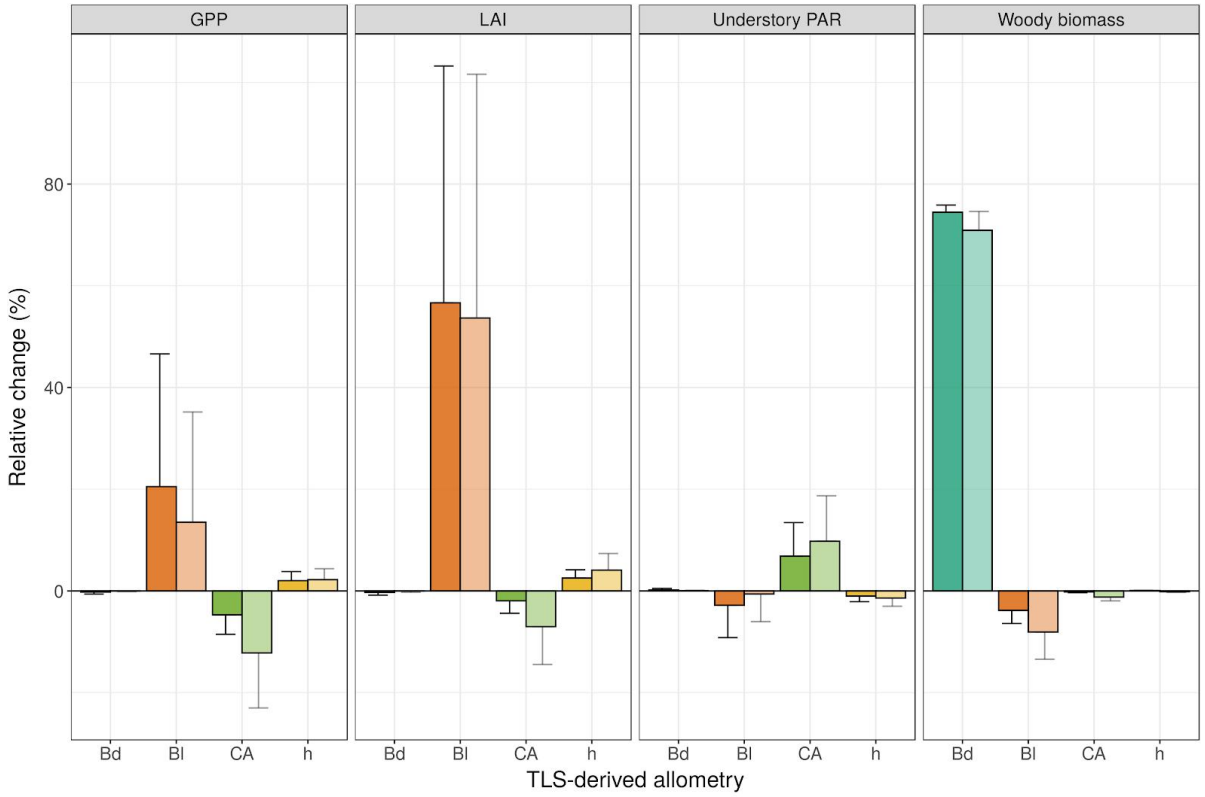

Figure 5: Relative impact of the TLS-derived allometries on several outputs of the ED2.2 model, when prescribed with initial conditions (Analysis II). For each allometry, direct and indirect (i.e. combined with one or several other allometries) changes are plotted as the dark and light bars, respectively. Bd, Bl, CA, and h respectively refer to the aboveground woody biomass, leaf biomass, crown area and height allometries (see Table 2).

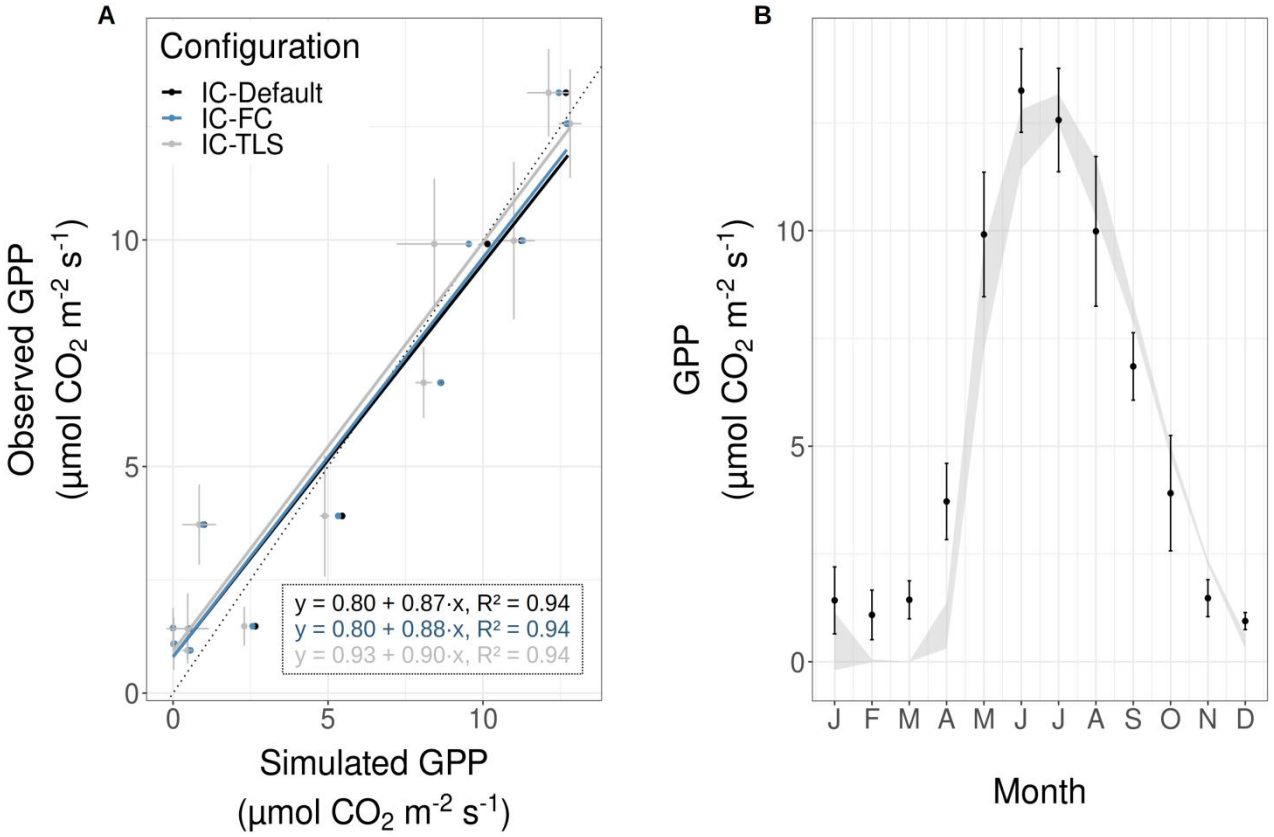

Figure 6: Goodness of fit for the Default (black), the finite crown (blue) and the TLS (grey) configurations (Analysis III). Model fitness is illustrated as observed vs modelled GPP (A) for all three configurations and as the seasonal cycle of modelled (grey, IC-TLS configuration only) and observed (black) GPP (B). The vertical error-bars of the measurements represent the mean ± one standard deviation of the observed flux for each month. The horizontal errorbars (A) and the shaded envelopes (B) encompass the mean ± one standard deviation of the 100 ensemble member posterior runs. For sake of clarity in subplot A, the errorbars are only shown for the IC-TLS configuration.

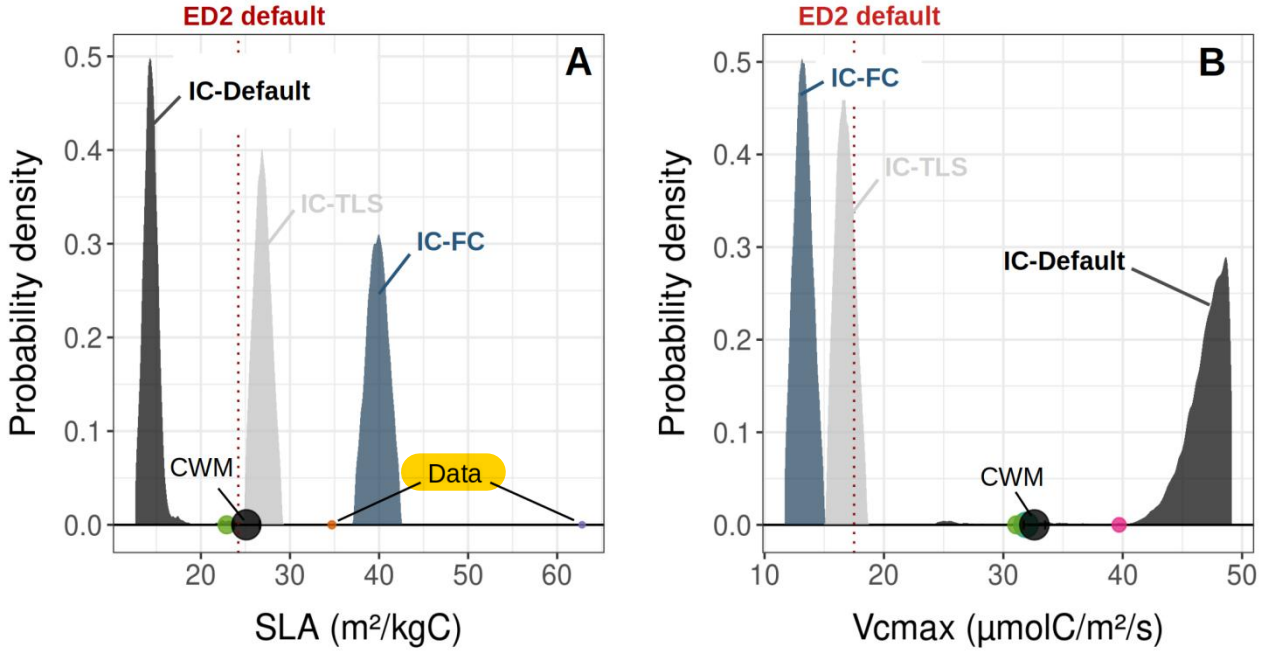

Figure 7: Posterior distributions of SLA (A) and V_{cmax} (B) when using the default allometries and inventory initial conditions (black), the inventory initial conditions and finite crown representation (blue) or the TLS-derived allometries and initial conditions (grey) to fit model parameters (Analysis III). Those distributions can be compared to the measured traits (coloured dots) and the community-weighted means (black dots). The radius of the dots is proportional to the basal area of the respective species (or the total basal area for the CWM) in the inventory (see also Table 1). The vertical dashed lines (red) indicate ED2.2 default values for both parameters.

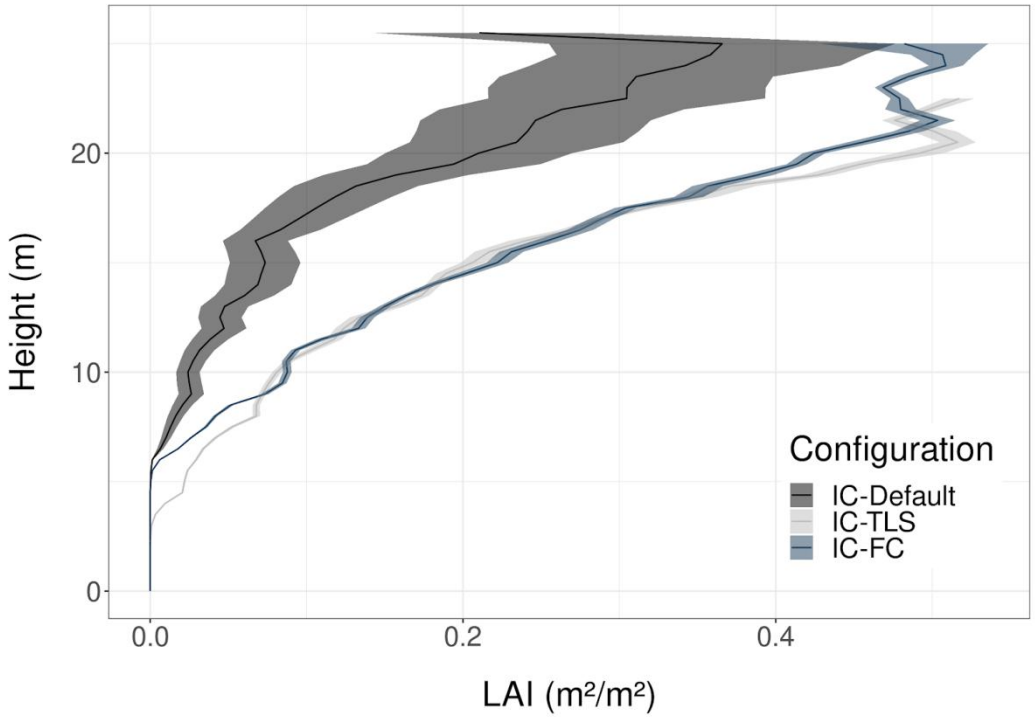

Figure 8: Ecosystem average vertical LAI distribution for the default configuration (black), the finite crown representation (blue), and the TLS (grey) posterior ensemble runs. The envelopes encompass the mean ± one standard deviation of the 100 ensemble member posterior runs.